Eur. Phys. J. D **18**, 93–111 (2002)
DOI: 10.1140/e10053-002-0012-9

THE EUROPEAN PHYSICAL JOURNAL D
EDP Sciences

Effective statistical weights of bound states in plasmas

D.V. Fisher[a] and Y. Maron

Faculty of Physics, Weizmann Institute of Science, Rehovot 76100, Israel

Received 10 August 2001

Abstract. Based on recent advances in the study of the statistics of interparticle distances and angles in plasmas, we develop an approach for the determination of the effective statistical weights of atomic (ionic) quantum states in ideal and nonideal plasmas. This approach allows one to account naturally for the effects of both the perturbation of the bound states by the neighboring ions and for the binding energy reduction due to the screening of the Coulomb interaction. We analyze the roles of tunneling and overbarrier escape of the optical electron from the parent ion potential well. The effects of neighbor ions and free electrons on these processes, and the simultaneous presence of several perturber ion species in the plasma are treated. We show that the present approach offers significantly more accurate effective-statistical-weight values in comparison to the existing theoretical treatments, and yields physical expressions for the empirical factors of the existing theories. Examples of calculations of effective statistical weights are given. The effects of the atomic (ionic) states collectivization on the collisional-radiative kinetics of dense plasmas are discussed.

PACS. 52.25.-b Plasma properties – 52.20.-j Elementary processes in plasmas

1 Introduction

A substantial progress has been recently achieved in controlled generation and time-resolved spectroscopy of dense plasmas (see *e.g.* Refs. [1–8]). However, the theoretical interpretation of experimental data, as well as the analysis of collisional-radiative kinetics in general, is still based on rather simplified treatments of plasma density effects. Almost exclusively, theoretical models of dense plasmas [9–11] utilize lowered-ionization-threshold (LIT) approximations like Debye-Hückel, Ion Sphere, or Stewart-Pyatt [12].

The main oversimplification inherent in all LIT approximations is the assumption that all atoms (ions) in a given ionization stage are immersed in an identical environment, *i.e.*, the statistics of spatial distribution of the neighboring perturber particles is not accounted for. As a consequence, the lowering of the ionization threshold is predicted to be the same for all atoms of a given ionization stage, and each bound energy level is predicted to become free abruptly in all the atoms as the LIT reaches it.

In reality, the number of the possible spatial arrangements of the perturber particles around a test atom (ion) in plasma is infinite, so every atom is found in different local conditions. In particular, there is always a finite probability that perturber ion(s) are located sufficiently close to the test atom for a given atomic bound state to become collectivized. For any atomic state this probability increases with the plasma density. Thus, as the density grows, a given bound atomic energy level does not disappear in all atoms at a certain threshold density as suggested by LIT approximations, but rather becomes increasingly scarce. It is, therefore, appropriate [13–19] to describe the plasma density effects on an atomic bound state q by introducing an Effective Statistical Weight (ESW) of that state:

$$g_q^{\mathrm{D}} = \omega_q g_q^0. \tag{1}$$

Here, the superscripts "D" and "0" refer to "atom in dense plasma" and "single atom in vacuum", respectively. For each atomic state, its bound (*i.e.*, non-collectivized) fraction ω_q decreases smoothly from 1 to 0 as the plasma density increases. At any given density, the higher is the atomic energy level the smaller is its bound fraction [13]. In the literature, ω_q is alternately called a "bound fraction" [13] or an "occupation factor" [18]. The two terms are strictly identical, as both refer to ω_q as defined by the equation (1); the term "bound fraction" suits better the atomic physics studies, while the term "occupation factor" – the equation-of-state studies. In this work, we choose to refer to ω_q as the "bound fraction".

So far, the ESW formalism has been utilized systematically only in equation-of-state and opacity calculations for the stellar interiors [20]. The primary reason for the ESW formalism being not generally used in the dense plasma research is the absence of accurate expressions for the bound fraction values. Even in steady-state plasmas the equations of state and the Rosseland opacities are sensitive to

[a] e-mail: fndima@plasma-gate.weizmann.ac.il

the exact ESW values of atomic and ionic states [21]. As we show in Section 6, in transient plasmas the sensitivity of the calculated bound state populations to the ω values used can be substantially stronger yet. It is thus highly important to conduct a detailed analysis of the effect of the dense plasma environment on the atomic and ionic states, and to derive accurate expressions for the bound fractions. Below we present a rigorous approach for the determination of ω_q in both ideal and nonideal plasmas. Our quantitative analysis is based on the recent progress in the study of the distributions of the neighbor ions around a neutral or charged ion in plasma [22]. The atom or ion under consideration is referred to as the "emitter ion". The plasmas are assumed to be classical and non-relativistic, *i.e.*, the temperature T_e of the free electrons is assumed to be much larger than their Fermi energy, but much smaller than $m_\mathrm{e}c^2 \approx 500$ keV.

The second goal of the present work is to develop a general description of quantum states of electrons in plasma on the basis of the ESW formalism. In the ESW formalism, the number density N_q of the ions in a state q only includes the ions in which q is not collectivized. Indeed, an electron, occupying the state q in an emitter ion in which that state is collectivized, can move freely between the emitter ion and the perturbing ions. Behavior of such an electron is similar to that of a truly-free (positive-energy) electron, and the electrons in the collectivized states are therefore included in the free electrons count. Consequently, the ESW formalism treatments used for practical calculations up to now [18,21] classify the electron states into two types only, namely, bound and free. In the pioneering works by Gündel [13,14] the electron states classification into three distinct types, namely, bound, quasi-free, and free, was suggested. However, Gündel has derived no benefit from that, since he considered only plasmas with Saha-Boltzmann equilibrium between the excited states and the ground state of the next ionization stage. Unfortunately, Gündel's results were never utilized for any purpose, as far as we know. In the present work we describe the bound, the collectivized, and the free electron states distinctively, and demonstrate the importance of the account for these three distinct types of the electron states in plasma. Our goal here is to develop a description for the electron states structure in plasmas, which would not be application-specific, but which would rather apply to the broad range of problems of plasma analysis, *e.g.* determination of plasma thermodynamic potentials, calculation of the ionization stage composition and quantum state abundances for equilibrium and transient plasmas, determination of the optical and transport coefficients, etc. In this work we suggest clear, universally applicable criteria for electron states classification into the three types.

The foremost issues in the present context are the thermodynamic consistency, and the continuity of the plasma composition and of the thermodynamic potentials as the functions of the macroscopic thermodynamic parameters. Both the continuity and the thermodynamic consistency requirements are satisfied naturally by the ESW description, as it has been explained in detail in references [18,23]. Thus, in the present work we concentrate primarily on the development of the detailed picture of the electron states and on the accurate determination of the ESWs of the bound states.

The rest of this paper is structured as follows. In Section 2 we present the basis of our approach and introduce the classification of the atomic (ionic) states into three types. In Section 3 we describe the distance scales at which various effects of the plasma environment on the optical electron states become significant. The scales hierarchy determined in Section 3 allows the relative importance of various effects produced by the surrounding charged particles to be readily compared further on. In Section 4 we describe our approach to ESW determination in detail, and present expressions for the ESWs. In Section 5 we compare our results to the results available in literature, and discuss the improvements achieved by the present approach in comparison to the existing theoretical treatments. In Section 6 we discuss and summarize the results obtained, describing the functional dependence of the ESWs on the macroscopic plasma parameters and outlining the effects of the electron states collectivization on the plasma collisional-radiative kinetics. In this work we make an extensive use of the 2-body (parent ion and its nearest neighbor (NN) ion) and 3-body (parent ion, NN ion, and next-nearest neighbor (NNN) ion) spatial distribution functions derived recently [22]. CGS units are used throughout this paper.

2 Three types of electron states in plasma

We classify the electron states in plasma into three types: bound, collectivized, and free. The free-electron states have energies $E > 0$, while both the bound and the collectivized states have energies $E \leq 0$. An optical electron is said to be bound when it is confined to the potential well of a single parent ion only. A negative-energy electron which moves freely between the potential wells of two or more neighbor ions (either above the potential barrier or by tunneling) is said to be collectivized. The energy E of an electron state in plasma differs from the energy of the corresponding state in an isolated ion due to the polarization of the plasma environment (Coulomb screening), see Section 4. At the beginning of Section 4 we present a strict criterion used to distinguish between bound and collectivized states.

In the ensemble of ions (atoms), throughout the domain $E < 0$ the bound and the collectivized states coexist. There is always a chance that the emitter ion in a certain state q has a perturber ion close enough to collectivize the state q, hence, in the ensemble of ions every state of the emitter optical electron is partially-collectivized. On the other hand, if in a given emitter ion some state q is collectivized, all the states q' above q in that *individual* ion are certainly collectivized, too. Ensemble-wise, this means that for every ionization stage of every chemical element the bound fraction ω_q is a monotonously-decreasing function of E, *i.e.*, a monotonously-increasing function

of the *binding* energy $E_{\rm bind}$ of the state q. For convenience, here and further on we characterize the bound and the collectivized states by a non-negative binding energy $E_{\rm bind} = -E \geq 0$.

In plasmas, besides the collectivization by neighboring ions there is an elimination of the sufficiently high-lying atomic (or ionic) states by free-electron screening. The screening eliminates the states for which the mean distance $\langle r \rangle$ between the optical electron and its parent ion is comparable to the screening radius $R_{\rm scr}$, *i.e.*, $\langle r \rangle$ is larger than the characteristic distance $a_{\rm e}$ between the free electrons[1]. The energy domain occupied originally by the eliminated states belongs in plasma to the free-electron continuum states, and the binding energies of the surviving atomic states (bound or collectivized) are accordingly reduced.

There exists a crucial difference in the effects of the two described phenomena (states collectivization and states elimination in plasma) on the electron states spectrum. This difference is manifested not in the spectrum of states of a single ion, but rather in the spectrum of states in the ensemble of ions. Optical electron energy spectrum in each *individual* atom or ion in plasma consists of bound states, collectivized states above them, and free electron states above the collectivized ones. The collectivization of a certain state of the emitter ion is governed by the spatial arrangement of individual neighbor ions around the emitter ion, and first of all by the distance from the emitter ion to its NN ion. Distance to the NN ion *varies* between individual atoms in plasma, and therefore any given state q is only collectivized in a fraction of atoms. Thus in an *ensemble* of atoms (ions) in plasma there is *no boundary* between the bound and the collectivized states, and all states can be regarded as partially-collectivized. The higher is the state, the larger is its collectivized fraction. The elimination of the high states by screening, on the contrary, involves the *collective* (rather than individual) effect of many free electrons and ions, and thus occurs *identically* for all atoms (ions) of the same charge. Hence, $E_{\rm bind}$ of any given state q is the same in every atom, and therefore for an ensemble of atoms in plasma the ionization threshold is well defined. The highest atomic states are fully collectivized, thus producing a smooth transition to the true free-electron continuum states.

It is important to note that the effects of the surrounding particles can not be separated completely into the ion-induced collectivization and the electron-induced screening. Indeed, the free electrons play a role in the collectivization of the atomic states by reducing their binding energy and by influencing the spatial distribution of the perturbing ions around the emitter. Conversely, the ions participate along with the free electrons in the screening of the Coulomb interactions in plasma. In our study of the dense plasma effects on the atomic states, and in the expressions for ω_q derived below, all the aforementioned contributions are taken into account.

[1] Of course, the condition $\langle r \rangle > a_{\rm e}$ is necessary but not sufficient for the atomic state elimination.

Following the ESW formalism convention, in this work we denote by N_q the population density of the bound fraction of the state q, *i.e.*, the number (per unit volume) of ions in which the state q is populated and bound. Number density of the ions in which the state q is populated and collectivized is included into the number density of the respective parent ions (*i.e.*, the ions obtained after the removal of the collectivized electrons). The free electron density $N_{\rm e} = N_{\rm c} + N_{\rm f}$ here is the sum of the densities of the collectivized electrons and of the free electrons proper, respectively. Consequently, the electroneutrality constraint is given simply by $N_{\rm e} = \sum_{Z_{\rm i}} Z_{\rm i} N_{Z_{\rm i}}$, where $N_{Z_{\rm i}}$ is the number density of the ions of the charge $Z_{\rm i}$ evaluated according to the above rules.

3 Hierarchy of interatomic distances

The main effects of the plasma environment on the optical electron quantum states are the Stark effect and, at higher densities, tunneling and overbarrier escape from the parent ion potential well. These effects are produced by the neighboring charged particles surrounding the emitter atom or ion considered, and are therefore governed by the relation of interatomic distances to the distance scales describing an optical electron wavefunction. Here we present the discussion of the interrelations between characteristic distances on the (inter)atomic scale, thus providing insight into the gradual change in the nature of ionic states with the increase of the plasma ion density or with changes in the plasma temperature and charge-state composition. The hierarchy of interatomic distances established, and the simple estimates presented in this section, will be utilized further in this work in the detailed study of the effects of neighbor particles on the emitter ion. Throughout this work, we denote by Z_0 the emitter *parent* ion charge, hence the emitter ion charge is $Z_0 - 1$. The charge of the perturber ion species considered is denoted $Z_{\rm i}$.

We first consider the case when the optical electron state, characterized by the principal quantum number n, has the binding energy value $E_{\rm bind}$ close to that of the hydrogen-like ion,

$$E_{\rm bind} \approx \frac{Z_0^2}{2n^2} \frac{e^2}{a_0}, \tag{2}$$

where a_0 is the Bohr radius. This approximation is good for hydrogen-like and helium-like ions, and for high excited states of any ion. For the low-lying states of the many-electron ions, expression (2) is inaccurate; such states will be considered at the end of this section.

The most useful spatial scale for the atomic bound state is the distance $r_{\rm class}$ from the parent ion core to the (outer) classical turning point of the optical electron "orbit". This distance is defined by the equality $Z_0 e^2 / r_{\rm class} = E_{\rm bind}$, *i.e.*,

$$r_{\rm class} = \frac{Z_0 e^2}{E_{\rm bind}} \approx \frac{2n^2}{Z_0} a_0. \tag{3}$$

The characteristic length $r_{\rm dec}$ of the exponential decay of the optical electron wavefunction inside the wall of the parent ion potential well (*i.e.*, beyond the outer classical turning point) is given by

$$r_{\rm dec} = \left(\frac{a_0 e^2}{2E_{\rm bind}}\right)^{1/2} \approx \frac{n}{Z_0} a_0 \approx \frac{r_{\rm class}}{2n}, \qquad (4)$$

see *e.g.* reference [24]. Hence, $r_{\rm dec}$ provides the smallest spatial scale of relevance to the problem at hand.

In the unperturbed atom, the optical electron is most likely to be found in the classically-allowed region, inside the parent potential well. The average distance $\langle r_n \rangle$ between the optical electron and its parent ion is therefore slightly smaller than the radius $r_{\rm class}$ of the classically-allowed region. Specifically, as long as the orbital momentum l of the optical electron is conserved,

$$\langle r_n \rangle \approx \frac{3n^2}{2Z_0}\left(1 - \frac{l\,(l+1)}{3n^2}\right) a_0$$

(see, *e.g.*, [24]; for hydrogen-like ions the equality is exact). For the states perturbed by an external electric field, however, l is not conserved, and therefore we simply use

$$\langle r_n \rangle \approx (1.0{-}1.5)\,\frac{n^2}{Z_0} a_0 \lesssim r_{\rm class} \qquad (5)$$

for further estimates.

So far we have considered a state n unperturbed by fields of surrounding particles. It is obvious that whenever there is a perturbing ion within roughly the distance $2r_{\rm class}$ from the parent ion, the optical electron prepared in the state n will no longer be bound to one ion, but rather will, with comparable probabilities, be found in the vicinity of at least two ionic cores. As said in the introduction, we consider such states collectivized.

Let us now study in detail the effect of the neighboring ions (and, later, electrons) on the optical electron quantum state. Consider the effect of the electric field produced by the perturbing ions at the parent ion location. This external field splits the state n of the optical electron into a manifold of Stark components (here we assume that the linear Stark effect dominates; the applicability range of this assumption will be discussed in the next section). The external field also lowers the potential barrier that confines the optical electron, eventually leading to a significant probability of the electron escape from the parent potential well. The motion of ions occurs on the time-scale much longer than that of the electrons, thus the ion fields may be treated as quasistatic (see, *e.g.*, Ref. [18]).

For the sake of discussion, let us first consider a single atom (or ion) under a slowly-increasing external field. The optical electron escape then occurs in a fully adiabatic way, which means that the electron escapes when the potential barrier peak reaches the unshifted energy level occupied by the optical electron (see, *e.g.*, Ref. [25]). This results in the condition for the critical electric field:

$$F_{\rm crit\ adiab} = \frac{E_{\rm bind}^2}{4Z_0 e^3} \approx \frac{Z_0^3}{16n^4}\frac{e}{a_0^2}\,. \qquad (6)$$

If we assume that this critical field is produced in plasma by the nearest perturber ion, we arrive at the following expression for the critical distance to this perturber ion:

$$R_{F_{\rm crit\ adiab}} \equiv \left(\frac{Z_{\rm i} e}{F_{\rm crit\ adiab}}\right)^{1/2} = \frac{4n^2 a_0}{Z_0}\left(\frac{Z_{\rm i}}{Z_0}\right)^{1/2}$$
$$\approx 2r_{\rm class} \quad \text{for} \quad Z_{\rm i} \approx Z_0. \qquad (7)$$

This is still, however, a rather crude estimate, since several important points were here disregarded. First, the local field is not uniform; it is actually much closer to the field of the nearest perturber ion, in the direction of which the escape of the optical electron really occurs. Second, there is no "slow increase of the external field" for an atomic electron in plasma. Instead, excitation or capture of an optical electron into a state n of the parent ion occurs in the presence of perturbing ions, and, provided the electron can escape from that state either by tunneling through or above the barrier, it escapes fast enough for the ionic configuration to remain essentially unchanged. With this in mind, the following conclusions seem logical: First, the effects of the NN ion both on tunneling and on overbarrier escape must primarily be looked at. Further on we will account for the effect of the NNN particles, and show that it is indeed much weaker. Second, one has to consider the electron escape from all the Stark components of the manifold n, since all of them may be collisionally populated in plasma; mixing within the manifold should also be taken into account. These observations allow us to amend the estimate (7): looking at the almost unshifted Stark components[2], considering the effect of the nearest perturber ion, and equating the barrier peak position to the binding energy of the level, we arrive at the following expression for the critical distance $R_{\rm crit.peak}$ to the nearest neighbor ion:

$$R_{\rm crit.peak} = \frac{2n^2}{Z_0}\left\{1 + 2\left(\frac{Z_{\rm i}}{Z_0}\right)^{1/2}\right\} a_0. \qquad (8)$$

Note that these considerations have led us to the expression obtained by Unsöld in his well-known "perturbing ion" model [26]. It is noteworthy that in the limit $Z_{\rm i} \gg Z_0$ the external field becomes nearly uniform, and the result approaches the uniform-field estimate (7). However, in the much more likely case $Z_{\rm i} \approx Z_0$ the critical distance becomes

$$R_{\rm crit.peak} \approx \frac{6n^2}{Z_0} a_0 \approx 3r_{\rm class} \quad \text{for} \quad Z_{\rm i} \approx Z_0, \qquad (9)$$

which is by factor 1.5 (corresponding to a factor 1.5^3 in density) larger than the estimate (7). This demonstrates the importance of accounting properly for the actual barrier shape. We also note that in sufficiently weakly coupled plasmas (those, to be specific, in which the ion microfield F distribution $P(F)$ is close to Holtsmark at least

[2] These are actually the majority of components, since for a given n the shift increases with $k = |n_1 - n_2|$ but the component degeneracy, given by $n - k$, decreases; here n_1 and n_2 are the parabolic quantum numbers.

in the $F \approx F_0$ domain, F_0 denoting Holtsmark normal fieldstrength) the typical uniform local microfield value found at the emitter ion location, *i.e.*, F_0, is nearly identical to the microfield produced at the same location by a neighbor ion found at the typical interionic distance

$$a = \left(\frac{4}{3}\pi N_{\rm i}\right)^{-1/3},$$

where $N_{\rm i}$ is the ion number density [27]. By contrast, the dependence of the local electric field strength on the position along the most likely escape path (the straight line connecting the emitter ion and the NN ion locations) differs significantly from that predicted in the uniform local microfield approximation. This demonstrates again the importance of the proper account not only for the electric field strength at the emitter location, but also for the spatial variation of electric field strength along the possible escape path of the optical electron. In the present work we account for the contributions of the individual ions to the distribution of the local potential in the vicinity of the emitter ion, thereby attaining a more accurate description of tunneling and overbarrier escape in plasma than available in literature up to now.

In plasmas of a single chemical element one usually finds $Z_{\rm i} \approx Z_0$. However, in plasmas of chemical mixtures $Z_{\rm i}$ can differ substantially from Z_0. Indeed, both in stellar and in laboratory plasmas the case of a high-Z impurity ion in a low-Z element plasma (Fe ion in H plasma, for example) is of great importance. In this case, Z_0 can be high (up to 26 for Fe) while $Z_{\rm i} = 1$ and the electrons are still non-relativistic. Then, the uniform local microfield approximation, expressions (6) and (7), yields

$$R_{F_{\rm crit\ adiab}} = \left(Z_{\rm i}\frac{4Z_0e^4}{E_{\rm bind}^2}\right)^{1/2} = \frac{2Z_0e^2}{E_{\rm bind}}\left(\frac{Z_{\rm i}}{Z_0}\right)^{1/2} = 2r_{\rm class}\left(\frac{Z_{\rm i}}{Z_0}\right)^{1/2}.$$

For $Z_{\rm i}/Z_0 < 1/4$, one finds $R_{F_{\rm crit\ adiab}} < r_{\rm class}$. The meaning of this inequality is as follows. In order to produce (at the emitter ion core location) a local field with a strength sufficient to permit the escape of the emitter ion optical electron above the potential barrier peak, the distance between the emitter ion core and the nearest perturber ion must be smaller than the radius of the potential well surrounded by that barrier! This means that the uniform local microfield approximation is inapplicable in this case, as the uniformity of the field fails completely on the distances about (or even smaller than) the optical electron wavefunction radius. On the other hand, the expression (8), obtained without the assumption of the local microfield uniformity, predicts $R_{\rm crit.peak} \gtrsim r_{\rm class}$ for $Z_{\rm i} \ll Z_0$, which is consistent with the physical picture of the overbarrier escape. We therefore arrive to the conclusion that in the limit $Z_{\rm i} \ll Z_0$ the states which have at least one perturber ion within the distance $r_{\rm class}$ from the emitter core should be considered collectivized. We note also that the aforementioned inequalities $R_{F_{\rm crit\ adiab}} < r_{\rm class}$ (for $Z_{\rm i}/Z_0 < 1/4$) and $R_{\rm crit.peak} \gtrsim r_{\rm class}$ remain valid even when $E_{\rm bind}$ does not obey (2), *i.e.*, for the low-lying states of the many-electron atoms as well.

Let us now consider the interionic distances that are significantly larger than $R_{\rm crit.peak}$. At such distances, the overbarrier escape of the optical electron is impossible, and the tunneling escape probability is negligible, but the Stark effect is still important. For high n, it is possible that even for distances to the nearest neighbor ion $R > R_{\rm crit.peak}$ the neighbor ion field will be sufficiently strong for the Stark manifolds n and $n+1$ to partially overlap (the level n is then found above the Inglis-Teller limit [25,28]). In this case, the spectral lines produced by the radiative decay from the levels n and $n+1$ can no longer be resolved, but the level n may still be effectively bound (see Ref. [12]), contributing to the abundance of the respective charge-state and to the collisional and radiative population and depopulation of the other energy levels. The distance $R_{\rm IT}$ to the NN ion at which the Stark manifolds n and $n+1$ of the emitter ion start to overlap is given by

$$R_{\rm IT} = a_0\left(Z_{\rm i}\frac{3n^5}{Z_0^3}\right)^{1/2} = (3n)^{1/2}\frac{n^2a_0}{Z_0}\left(\frac{Z_{\rm i}}{Z_0}\right)^{1/2} \approx \frac{\sqrt{3n}}{2}r_{\rm class},$$

up to the lower-order terms in n. Comparing $R_{\rm IT}$ to $R_{\rm crit.peak}$ we find that, in the case of the perturbation by the NN ion, only for $n \gtrsim 10$ the n and $n+1$ Stark manifolds can overlap while most of the n manifold is still under the barrier peak. If the perturbation is caused by a uniform external field, then, by contrast, the underbarrier overlap can occur already for $n = 4$. Here, again, the importance of the proper account for the potential barrier profile becomes apparent.

For the low-lying states of many-electron atoms the approximation (2) fails, but the hierarchy of the distances remains the same. Indeed,

$$r_{\rm class} = \frac{Z_0e^2}{E_{\rm bind}},$$

$$r_{\rm dec} = \left(\frac{a_0e^2}{2E_{\rm bind}}\right)^{1/2} < r_{\rm class}$$

since $E_{\rm bind} < 2Z_0^2\dfrac{e^2}{a_0}$ for any optical electron state,

$$\langle r_n\rangle \lesssim r_{\rm class}, \tag{10}$$

$$R_{F_{\rm crit\ adiab}} = \frac{2Z_0e^2}{E_{\rm bind}}\left(\frac{Z_{\rm i}}{Z_0}\right)^{1/2} \approx 2r_{\rm class},$$

$$R_{\rm crit.peak} = \frac{Z_0e^2}{E_{\rm bind}}\left\{1 + 2\left(\frac{Z_{\rm i}}{Z_0}\right)^{1/2}\right\} \approx 3r_{\rm class}. \tag{11}$$

Evidently, the Inglis-Teller criterion is inapplicable in this case.

The analysis above establishes the hierarchy of the microscopic distance scales in plasmas and demonstrates the

importance of account for the *spatial variation* of the local electric field *in the vicinity* of the emitter ion location (rather than just for distribution $P(F)$ of the local electric field strength *at* the emitter ion location) for an accurate treatment of the plasma density effects on ionic states.

4 Determination of the effective statistical weights

4.1 Collectivization of atomic (ionic) states

We start by giving a strict formulation of the difference between the bound and the collectivized states. Consider an electron occupying a certain quantum state in its parent ion potential well. The electron can leave this state either by transition (namely, by spontaneous radiative decay, impact or radiative excitation, deexcitation or ionization), or by moving away from its parent ion into the potential well(s) of the neighbor ion(s) without a change in its energy. In the first case we can speak of the *motion along the energy axis* while in the second case we can speak of the *motion in space only*.

Consider now a certain spatial arrangement of perturber ions around the emitter ion. For each energy level q of the emitter-ion optical electron it is, in principle, possible to determine whether that level is situated above the potential barrier separating the potential well of the parent ion from the potential wells of the neighboring ions (along the path where the barrier is most depressed). If q is above the barrier, then the optical electron will have comparable probabilities to be close to the neighbor ion or close to the parent ion, therefore, the state q is collectivized. The identification of the above-barrier states as collectivized (*i.e.*, no longer bound to a single ion) is well-established [13,18,26,29]. Still, we will further discuss this definition in order to consider possible caveats. Not all the below-barrier states, on the other hand, can be identified as bound. Indeed, it was mentioned already by Unsöld [26] that the states lying below the potential barrier peak are affected by tunneling. Returning to our picture of the motion along the energy axis *versus* the motion along the spatial axis, the following conclusion is readily reached: a below-barrier state must be deemed collectivized when its depopulation by tunneling is more likely than its depopulation by transitions (spontaneous, impact- or radiation-induced) to other states.

We emphasize the fact that the populations of high-lying states in a dense plasma are generally found in the Saha-Boltzmann equilibrium between themselves and the ground state of the higher ionization stage [12,30,31]. This is true both for bound and for collectivized states. Indeed, the tunneling does not reduce the population of a state; instead, it provides channels for both its population and depopulation. For transient plasmas, however, the difference in the dominant population-depopulation mechanism between the bound and the collectivized states is important. Indeed, the collectivized states are populated and depopulated by tunneling or overbarrier electron motion, *i.e.*, generally, by the motion of the electrons in the field of the surrounding particles, similarly to the free electron states. Populations of the collectivized states, therefore, reach equilibrium with the population of the ground state of the higher ionization stage on the time scale comparable to the time scale of Maxwellization of the free electron subsystem. This time can be significantly shorter than the time required for the high-lying bound states to reach Saha-Boltzmann equilibrium. Transitions involving collectivized states may therefore affect decisively the transient plasmas composition. This subject will be further discussed in Sections 5 and 6.

We consider an emitter ion of charge $Z_0 - 1$ and its NN perturber ion of charge Z_i. The emitter ion is in a quantum state q. Let us denote by R_q the critical distance between the emitter ion and the NN ion, *i.e.*, the maximum distance at which the perturber ion causes the collectivization of the state q. Since there are two possible mechanisms of the optical electron collectivization, namely, overbarrier-escape and tunneling, the distance R_q is the larger of the two critical distances:

$$R_q = \max\left\{R_{\mathrm{crit.peak}}, R_{\mathrm{tunn}}\right\}, \tag{12}$$

where R_{tunn} is the critical distance at which the optical electron is collectivized by tunneling. Once $R_q(Z_\mathrm{i})$ is known, the fraction of the emitter ions in which the state q is bound is readily evaluated. It is, by definition, given by the probability of *no* perturber ions of charge Z_i being located within R from the emitter ion. Denoting by $P_0(R)$ the probability for having no ions (of the charge Z_i) within the distance R from the emitter ion, we therefore identify

$$\omega_q = P_0(R_q). \tag{13}$$

The case when several perturber species coexist in plasma is considered further on. The probability distribution $P_0(R)$ has been derived in reference [22]. It is given by

$$P_0(R) = \exp\left[-4\pi N_{Z_\mathrm{i}} \int_0^R r^2 \mathrm{d}r \exp\left\{-\frac{Z_\mathrm{i} e U_{\mathrm{NN}}(r)}{T}\right\}\right], \tag{14}$$

where $U_{\mathrm{NN}}(R)$ is the potential experienced by the NN ion at the distance R from the emitter ion. Equality of electron and ion temperatures, $T_\mathrm{e} = T_\mathrm{i} = T$, is assumed here for convenience. For the plasmas with an ion-ion coupling parameter

$$\Gamma_{\mathrm{ii}} = \frac{Z_0 Z_\mathrm{i} e^2}{aT} \approx \frac{Z_0^2 e^2}{aT} \tag{15}$$

in the range $0 \leq \Gamma_{\mathrm{ii}} < 1$, reference [22] shows that $U_{\mathrm{NN}}(R)$ is well approximated by

$$U_{\mathrm{NN}}(R) = \frac{e}{R}\left(Z_0 - 1 - \frac{4}{3}\pi R^3 Z_\mathrm{i} N_{Z_\mathrm{i}}\right)\exp\left(-R/R_\mathrm{D}\right), \tag{16}$$

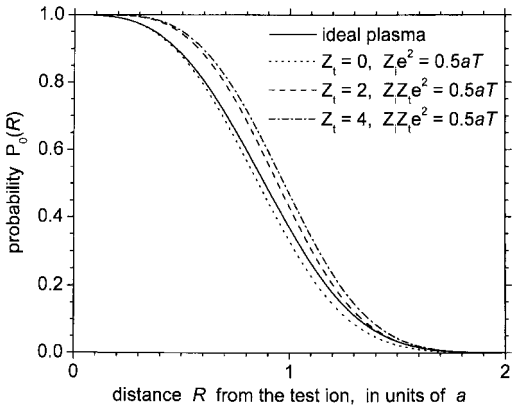

(a)

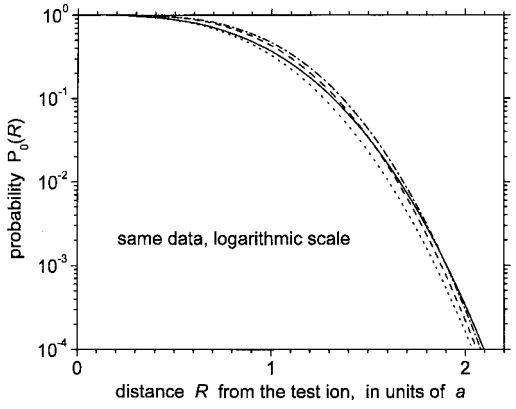

(b)

Fig. 1. (a) Probability $P_0(R)$ to find no ions of charge Z_i within the distance R from the test ion of charge $Z_\mathrm{t} = Z_0 - 1$, shown for various values of Z_t and Γ. For all four curves $Z_\mathrm{i} = 2$. Note that at the short distances the direct ion-ion repulsion results in the values of $P_0(R)$ being much closer to 1 for a positive test ion than for a neutral test ion or for an ideal plasma. The ideal plasma limit of $P_0(R)$ is simply $P_0^{\mathrm{id}}(R) = \exp\left\{-(R/a)^3\right\}$. (b) Same data as in (a), presented on a logarithmic scale. Note that at $R/a \gtrsim 1$ the electron-ion interactions become important, resulting in the lower values of $P_0(R)$ for nonideal plasmas than for an ideal plasma at these distances (in contrast to the short-distance behavior).

where R_D is the Debye radius. The replacement of the term $Z_0 - 1$ by the function $\tilde{Z}_\mathrm{t}(R)$ introduced in reference [22] provides some further improvement in accuracy at the expense of versatility.

Figure 1 illustrates the dependence of $P_0(R)$ on the plasma conditions. The rest of the present section is primarily focussed on the derivation of accurate expressions for the critical distance R_q. The functional dependence of ω_q on the macroscopic plasma parameters (*via* P_0 and R_q) is summarized in the first part of Section 6.

In reference [22] it was also shown that, for the purpose of determination of the spatial distributions of the neighbor ions in the vicinity of an emitter ion in plasma, the neighbor ions may reliably be considered pointlike. Thus, the perturber ions may be described by their charge Z_i only[3]. In the case when perturber ions with different values of Z_i coexist in plasma, the bound fraction is given by the probability to have no ions of *any* charge Z_i within the respective critical distances $R_q(Z_\mathrm{i})$. Assuming the absence of correlation between the perturbers of different Z_i, we obtain

$$\omega_q = \prod_{Z_\mathrm{i}} P_0\left(R_q\left(Z_\mathrm{i}\right)\right), \tag{17}$$

where both the function $P_0(R)$ and the value of R_q depend on Z_i.

4.2 Basis of the present approach

As it was already said, a change in the nature of an electron state, from being a bound state of a single ion in dilute plasmas to encompassing several ions in dense plasmas, is closely related to the possibility of the escape of an optical electron out of the parent ion potential well [16,18,26,29]. The low-frequency component [18] of the microfield produced at the atom (ion) location by the surrounding charged particles can lower the atomic potential barrier sufficiently for an atomic electron either to tunnel out of its potential well or to escape above the peak of the lowered potential barrier. The two approximations most commonly used to describe the escape of the optical electron from its parent ion in plasmas are the Uniform Local Microfield (ULM) approximation and the Nearest Neighbor approximation, both dating back to the original Unsöld paper [26]. The difference between the two approximations is in the assumed spatial dependence of the field acting on an atom. In the ULM approximation, the local microfield is assumed to be constant across the potential barrier that the optical electron tunnels through, and equal to the microfield found at the parent ion location. In the NN approximation, the local microfield is assumed to be produced by the NN ion, and thus increases significantly across the potential barrier (along the tunneling path, which is the straight line connecting the parent and the NN ions). Note that the ULM method takes into account the collective effect of the surrounding ions, while the NN method only describes the effect of the nearest one. However, as seen above, the NN method describes the shape of the potential barrier with significantly higher accuracy than the ULM method.

In order to determine accurately the ESWs of the bound states, the effect of the individual perturbing particles must be accounted for, thus avoiding the drawbacks of both ULM and NN approximations. We choose to take the NN approach as the starting point, expressing ω_q in terms of the critical distance R_q. However, in contrast to

[3] Perturber ions of different chemical elements or isotopes may, of course, have the same charge but different masses. However, perturber ion mass does not enter any of the statistical quantities considered. Thus, here N_{Z_i} is the total number density of all the ions of charge Z_i available in plasma.

the traditional approach, in our treatment R_q is a function of the positions of the other surrounding particles (besides the NN ion) around the emitter ion. The potential produced by all the perturbing particles (ions and free electrons) around the emitter ion can be conveniently represented as a sum of three terms:

(i) the NN ion potential,
(ii) the ensemble average of the total potential of the other perturbing particles (OPP),
(iii) and the stochastic deviations of the total OPP potential from its average value. The last term decomposes into the ionic component (discussed in this section) and the free-electron component (discussed in Sect. 5).

In the traditional NN approach, out of the above three terms only the term (i) is considered. In reality, both the average and the stochastic part of the total OPP potential, being superimposed on the potential of the emitter and NN ions, alter the potential barrier height and shape and thus influence the values of $R_{\mathrm{crit.peak}}$ and R_{tunn}.

The average part of the OPP potential, term (ii), is the screening potential. Its primary effect is in the reduction of the binding energy of the optical electron in emitter ion. This reduction is identical for all emitter ions of the same charge. The stochastic part of the OPP potential, term (iii), on the other hand, causes a bias of the potential barrier, *i.e.*, a shift of the optical-electron energy level with respect to the peak of the potential barrier between the emitter ion and the NN ion. This shift is different for different individual emitter ions, therefore, on average, it corresponds to the broadening of the level. Note that we do not describe this as the Stark effect. Indeed, the Stark effect is produced by all the surrounding particles, and the respective contributions of the NN ion and of the OPP to the Stark effect are not distinguished. Here, on the contrary, we distinguish between the effects of the NN ion and of the other particles. The bound fraction value ω_q is governed by the critical distance R_q to the NN ion, while the level broadening produced by the term (iii) of the surrounding particles potential manifests itself in the "broadening", *i.e.* smearing, of the R_q value. Besides that, the term (iii) breaks the axial symmetry of the potential given by the terms (i) and (ii). Indeed, in absence of the term (iii) the potential experienced by the optical electron is axially symmetric with respect to the line connecting the emitter ion and the NN ion. Below we demonstrate the significance of this symmetry breaking, and account for it.

We derive the expressions for $R_{\mathrm{crit.peak}}$ in Sections 4.3 and 4.4, and the expressions for R_{tunn} in Section 4.5. These expressions are obtained taking into account the terms (i) and (ii) of the perturbing potential. In Section 4.6 we account in detail for the effects of screening by the surrounding particles, and provide expressions for the binding energy reduction in both ideal and nonideal plasmas. The effects produced by the ionic component of the term (iii) of the perturbing potential, and their influence on $R_{\mathrm{crit.peak}}$ and R_{tunn}, are treated in Section 4.7. The effects of the free-electron component of the term (iii) are discussed in Section 5.

4.3 Barrier peak

We consider the potential barrier profile along the straight line connecting the emitter ion with its NN ion. Let us denote the distance between the two ions by R, and a position on the line connecting the ions by r. On the segment $0 \leq r \leq R$, the potential is dominated by the potentials of the emitter parent ion and of the NN ion,

$$V(r) = -\frac{Z_0 e}{r} - \frac{Z_{\mathrm{i}} e}{R - r}.$$

We start our consideration of the optical-electron overbarrier escape with this simple expression for potential, which corresponds to the term (i) of the total potential introduced in the previous subsection. We take into account the term (ii) of the total potential (collective screening effect of the OPP) by using the effective binding energy of an optical electron near its parent ion in plasma, which is given by

$$E_{\mathrm{bind}}^{\mathrm{eff}} = E_{\mathrm{bind}}^{0} - \Delta E(N_{\mathrm{e}}, T_{\mathrm{e}}). \tag{18}$$

Here $E_{\mathrm{bind}}^{0} > 0$ is the binding energy in an isolated emitter ion, and $\Delta E(N_{\mathrm{e}}, T_{\mathrm{e}})$ is the reduction of the binding energy due to the polarization of the surrounding cloud of free electrons and ions in plasma. The expressions for $\Delta E(N_{\mathrm{e}}, T_{\mathrm{e}})$ are presented in Section 4.6. The term (iii) of the total potential is taken into account in Section 4.7.

The peak of the barrier is located at

$$r_{\mathrm{peak}} = R\frac{Z_0 - \sqrt{Z_0 Z_{\mathrm{i}}}}{Z_0 - Z_{\mathrm{i}}}.$$

The value of potential at the barrier peak is given by

$$V_{\mathrm{peak}} = -\frac{\left(\sqrt{Z_0} + \sqrt{Z_{\mathrm{i}}}\right)^2 e}{R}. \tag{19}$$

Taking into account the zero-order down shift of all energy levels by $Z_{\mathrm{i}} e^2/R$, but neglecting for now the Stark effect, the critical distance $R = R_{\mathrm{crit.peak}}^{(0)}$, at which the energy level touches the barrier peak, may be found from the equation

$$E_{\mathrm{bind}}^{\mathrm{eff}} + Z_{\mathrm{i}} e^2/R + V_{\mathrm{peak}}(R)\, e = 0. \tag{20}$$

The superscript 0 of $R_{\mathrm{crit.peak}}^{(0)}$ shows that only the zero-order shift was taken into account. Equation (20) gives

$$R_{\mathrm{crit.peak}}^{(0)} = \frac{Z_0 + 2\sqrt{Z_0 Z_{\mathrm{i}}}}{E_{\mathrm{bind}}^{\mathrm{eff}}} e^2. \tag{21}$$

Let us now take the Stark effect into account. For the emitter bound state belonging to the term $(L_P S_P)\, nlLS$, where L_P, S_P and L, S are the total orbital momentum and the spin quantum numbers of the parent ion and of

$$R^{(1)}_{\rm crit.peak} = \frac{Z_0 + 2\sqrt{Z_0 Z_{\rm i}} + \sqrt{\left(Z_0 + 2\sqrt{Z_0 Z_{\rm i}}\right)^2 + 6E^{\rm eff}_{\rm bind} n\,(n_1 - n_2)\,\frac{Z_{\rm i}}{Z_0}\,\frac{a_0}{e^2}}}{2E^{\rm eff}_{\rm bind}} e^2 \tag{23}$$

$$\langle n_1, n_2, m\,|V_{\rm NN} e|\, n_1, n_2, m\rangle = \frac{(n_1+|m|)!\,(n_2+|m|)!}{2n^4\,(|m|!)^4\,n_1!n_2!} Z_0^3 e \int_0^\infty {\rm d}\eta \int_0^\infty {\rm d}\xi\,(\eta+\xi)\,V_{\rm NN}(\eta,\xi)$$
$$\times F^2\left(-n_1, |m|+1, \frac{Z_0\xi}{n}\right) F^2\left(-n_2, |m|+1, \frac{Z_0\eta}{n}\right)\left(\frac{Z_0^2\eta\xi}{n^2}\right)^{|m|} \exp\left(-Z_0\frac{\eta+\xi}{n}\right),$$

the emitter, respectively, it would be, generally speaking, incorrect to apply the expression for linear Stark shifts developed for a hydrogen-like ion. However, one must realize that the state we are interested in is *a priori* strongly perturbed by the field of the NN ion, and l is certainly not conserved. Therefore, we assume now the applicability of the expressions for the linear Stark shifts, postponing the discussion to the end of the present subsection. The values of the linear Stark shifts of an electron state with the principal quantum number n are given, for example, in reference [24]. Accounting for these shifts, the equation (20) for $R = R^{(1)}_{\rm crit.peak}$ assumes the form

$$E^{\rm eff}_{\rm bind} + \frac{Z_{\rm i}e^2}{R} - \frac{3}{2Z_0} n\,(n_1 - n_2)\,\frac{Z_{\rm i}e^2 a_0}{R^2} - V_{\rm peak}(R)\,e = 0, \tag{22}$$

where $V_{\rm peak}(R)$ is given by expression (19), and (n_1, n_2, m) are the parabolic quantum numbers describing the given Stark component belonging to the manifold n. Note that in this notation m can be negative. From (19) and (22) one readily finds

see equation (23) above.

Obviously, the individual Stark components have different values of $R_{\rm crit.peak}$. This implies that, for a given ion density, there will be different bound fractions for the different Stark components of the same level n. Namely, the most-red, *i.e.* lowest-lying component, $n_2 = n-1$, will have the smallest value of $R_{\rm crit.peak}$ and therefore the largest bound fraction $\omega_{n_1,n_2,m}$. The bound fraction of the entire level n must be weighted over the components:

$$\omega_n = n^{-2} \sum \omega_{n_1,n_2,m}\ , \tag{24}$$

where the summation is over all the Stark components of the level n.

Validity of the linear Stark effect approximation needs to be verified in this case, since the NN ion field is not uniform. To find the more accurate values of the bound state shifts in presence of the NN ion, we have performed the first-order perturbation theory calculations of the level shifts. Following reference [24], we find the shifts to be given by

see equation above

where

$$V_{\rm NN}(\eta,\xi) = -\frac{Z_{\rm i}e}{\sqrt{R^2 + R\,(\xi-\eta) + \frac{1}{4}\,(\xi+\eta)^2}}$$

is the NN ion potential in the parabolic coordinates, and $F(k_1, k_2, x)$ is the confluent hypergeometric function. The integral is readily evaluated numerically. We have found that at the interionic distances $R \approx R^{(0)}_{\rm crit.peak}$ being considered, the calculated shift values are approximated by the linear Stark effect values

$$\langle n_1, n_2, m\,|V_{\rm NN} e|\, n_1, n_2, m\rangle \approx -\frac{Z_{\rm i}e^2}{R} + \frac{3}{2Z_0} n\,(n_1 - n_2)\,\frac{Z_{\rm i}e^2 a_0}{R^2}$$

to within 10% (and mostly to within 3%) accuracy at least for $n \lesssim 25$ and $Z_0 \sim Z_{\rm i}$, *i.e.*, over the entire domain considered. Even a 10% error in the Stark shifts corresponds to an error of about 1% or less in $R^{(1)}_{\rm crit.peak}$. Thus, expression (23) indeed yields accurate values of the critical distances.

Let us now consider the criterion for the inclusion of the linear Stark effect in the calculations. Clearly, for the hydrogen and hydrogen-like ions the Stark effect is linear even at weak fields, and must be included. For low ionization stages of high-Z elements, on the other hand, the existence of a large quantum defect necessitates the individual account for the s- and possibly p-states of the optical electron, since the binding energies of these states exceed significantly the binding energies of the high-l states of the same n. In such a case the bound fraction of the s-state may be significantly larger than the bound fractions of the high-l states of the same n. We suggest to use the following simple criterion for the inclusion of the linear Stark effect in the ESW calculations: if, for the given value of n, the energy difference between the outermost Stark components

$$\varepsilon \approx \frac{3n\,(n-1)}{Z_0}\,\frac{Z_{\rm i}e^2 a_0}{R^2_{\rm crit.peak}} \approx \frac{n-1}{12n^3} Z_0^2 \frac{e^2}{a_0} \quad \text{for} \quad Z_{\rm i} \approx Z_0$$

exceeds the energy difference between the highest and the lowest unperturbed energy level of the optical electron

in the configuration considered, then it is best to take the linear Stark effect into account for this configuration. Then, ω_n is evaluated using (24) and the same value of $\omega = \omega_n$ is ascribed to all the terms of this configuration. In the opposite case, the linear Stark effect should not be included in the calculations. Then, the individual bound fractions ω_q may be introduced for every term (or level) q using $R_q = R^{(0)}_{\rm crit.peak}$ evaluated for the corresponding value of $E^{\rm eff}_{\rm bind}$. Saying "configuration" here we imply not only the specified value of the principal quantum number n of the optical electron, but also the parent ion configuration *and* term $(n_1 l_1)^{i_1} \ldots (n_k l_k)^{i_k} L_P S_P$, where k is the number of nl-subshells filled completely or partially by the parent ion bound electrons. The unperturbed optical electron binding energy $E^0_{\rm bind}$ for the term $(L_P S_P)\, nlLS$ is defined, of course, as the threshold energy for the ionization process in which the ion in the term $L_P S_P$ is produced. For the fractional parentage case, the peculiarities of the field ionization process are considered in reference [32].

4.4 Role of the linear Stark effect

Let us now consider the role of the linear Stark term in the equation (22) for the determination of ω_n. For the most-red and most-blue Stark components, namely $(n_1 = 0,\ n_2 = n-1,\ m = 0)$ and $\big(n_1 = n-1,\ n_2 = 0,\ m = 0\big)$, the linear Stark shift has a significant effect on $\omega_{n_1,n_2,m}$. However, this does not at all imply that the linear Stark shifts should affect significantly the result (24) for ω_n as well. The reason for that is twofold. First, the majority of the n level components have $|n_1 - n_2|$ notably smaller than n, and do not exhibit large linear Stark shifts. Second, the differences between $R^{(1)}_{\rm crit.peak}$ for the most-red component and $R^{(1)}_{\rm crit.peak}$ for the central components, and between $R^{(1)}_{\rm crit.peak}$ for the most-blue component and $R^{(1)}_{\rm crit.peak}$ for the central components, are opposite in sign and (in the first order) have the same absolute value. In general, for components of the same Stark manifold n the difference

$$R^{(1)}_{\rm crit.peak}(n_1, n_2, m) - R^{(1)}_{\rm crit.peak}(n_1 = n_2)$$

is approximately proportional to $(n_1 - n_2)$. The dependence of $\omega_{n_1,n_2,m}$ on $R^{(1)}_{\rm crit.peak}(n_1, n_2, m)$ is given by expression (13). As long as $R^{(1)}_{\rm crit.peak}(n_1 = n_2) < a$, *i.e.*, as long as ω_n is comparable to 1, the variation of $R^{(1)}_{\rm crit.peak}(n_1, n_2, m)$, say by about 10%, does not produce a drastic change in $\omega_{n_1,n_2,m}$ (the response of $\omega_{n_1,n_2,m}$ to such variations of $R^{(1)}_{\rm crit.peak}(n_1, n_2, m)$ in this case is, if not completely linear, still dominated by the linear term). The linear terms in the response of $\omega_{n_1,n_2,m}$ and $\omega_{n_2,n_1,m}$ to the deviations of $R^{(1)}_{\rm crit.peak}(n_1, n_2, m)$ and $R^{(1)}_{\rm crit.peak}(n_1, n_2, m)$, respectively, from $R^{(1)}_{\rm crit.peak}(n_1 = n_2)$, cancel out. This results in further suppression of the effect of the linear Stark shifts on ω_n.

By contrast, when $R^{(1)}_{\rm crit.peak}(n_1 = n_2) > 2a$, *i.e.*, when $\omega_n \ll 1$, the dependence of $\omega_{n_1,n_2,m}$ on $R^{(1)}_{\rm crit.peak}(n_1, n_2, m)$ is highly nonlinear, *i.e.*, a 10% variation in $R^{(1)}_{\rm crit.peak}(n_1, n_2, m)$ can change $\omega_{n_1,n_2,m}$ by several orders of magnitude. Thus, the sum (24) is in this case dominated by the single term corresponding to $\omega_{n_1,n_2,m}$ of the most-red component, $n_2 = n-1$, and therefore the linear Stark effect starts to play a decisive role as ω_n becomes very small.

4.5 Tunneling

In the case when $R > R_{\rm crit.peak}$, the optical electron of the emitter atom (ion) can still escape from its parent potential well by tunneling through the potential barrier in the place where the barrier is thinnest. Let us now determine the critical distance $R_{\rm tunn}$. As we said above, the quantum state q of the emitter ion is considered collectivized by an arrangement of perturber ions around the emitter when the probability for the optical electron to leave the emitter ion by tunneling is higher than the probability for it to undergo a collisional or a radiative (CR) transition. We denote the total probability, per unit time, of CR transitions from q (sum over all channels, both bound-bound and bound-free) by $\Gamma^{\rm CR}_q$, and the tunneling probability per unit time by $\Gamma^{\rm tunn}_q$. While $\Gamma^{\rm CR}_q$ does not depend strongly on the spatial arrangement of the perturbers, $\Gamma^{\rm tunn}_q$ is a sharply decreasing function of the distance R to the nearest perturber ion. Comparing the probabilities, we can thus neglect the dependence of $\Gamma^{\rm CR}_q$ on the perturber positions. The probabilities $\Gamma^{\rm tunn}_q(R)$ and $\Gamma^{\rm CR}_q$ are of the same order only in a narrow range of R near $R_{\rm tunn}$, where $R_{\rm tunn}$ is defined by the equation

$$\Gamma^{\rm tunn}_q(R_{\rm tunn}) = \Gamma^{\rm CR}_q. \tag{25}$$

For the given state q, for $R > R_{\rm tunn}$ the CR processes dominate, whereas for $R < R_{\rm tunn}$ the state q is mainly populated and depopulated by tunneling. Thus, the bound fraction ω_q is in this case the fraction of atoms that have no perturbers closer than $R_{\rm tunn}$. Therefore, it is given by expression (13) with $R_q = R_{\rm tunn}$. It is important to note that, since $\Gamma^{\rm tunn}_q(R)$ decreases sharply with R in the region $R \gtrsim R_{\rm crit.peak}$ due to the exponential dependence on the action across the potential barrier [24], the value of $R_{\rm tunn}$ given by equation (25) depends weakly on the values of $\Gamma^{\rm tunn}_q$ and $\Gamma^{\rm CR}_q$. Typically, a factor of 10 change in $\Gamma^{\rm tunn}_q$ or $\Gamma^{\rm CR}_q$ results in only a 10–20% change in $R_{\rm tunn}$. It is thus unnecessary to determine $\Gamma^{\rm tunn}_q$ with high accuracy (except, possibly, in the $\omega_q \ll 1$ domain where $P_0(R_q)$ decreases sharply with R_q; but calculations show that when ω becomes small the overbarrier escape takes over and tunneling becomes unimportant).

In this work, we use the expressions for the probability $\Gamma^{\rm tunn}_q(R)$ of tunneling between the two Coulomb potential wells derived by Grozdanov and Janev [33]. Their expressions for $\Gamma^{\rm tunn}_q(R)$ were obtained by directly solving the Schrödinger equation, and are exact in the limit of large R.

However, in the region $R \gtrapprox R_{\text{crit.peak}}$ the potential barrier is already thin, and the results for $\Gamma_q^{\text{tunn}}(R)$ are only approximate. Indeed, the expressions for $\Gamma_q^{\text{tunn}}(R)$ in [33] correspond to the expansion in the small parameter

$$\frac{n^2 a_0}{Z_0 R}\sqrt{\frac{2Z_\text{i}}{Z_0}} \ll 1,$$

while in our case

$$\frac{n^2 a_0}{Z_0 R}\sqrt{\frac{2Z_\text{i}}{Z_0}} \lessapprox \frac{n^2 a_0}{Z_0 R_{\text{crit.peak}}}\sqrt{\frac{2Z_\text{i}}{Z_0}} \approx 0.2.$$

However, as said above, high accuracy of Γ_q^{tunn} is not required for our purposes, and thus the expressions derived in reference [33] can be used.

Here, as in Section 4.3, we encounter the two possible cases: the optical-electron energy-level splitting is either dominated by the linear Stark effect or by the splitting on l. In the case when the linear Stark effect is dominant, the expression (20) of reference [33] is directly applicable for the determination of $\Gamma_q^{\text{tunn}}(R)$ of the individual Stark components. The bound fractions $\omega_{n_1,n_2,m}$ of the Stark components of the level n are found solving equation (25) above for R_{tunn} and using (12), (13) for $\omega_{n_1,n_2,m}$. The bound fraction of the level n is then found using our expression (24). Since it is impractical to determine the transition probabilities $\Gamma^{\text{CR}}_{q=(n_1,n_2,m)}$ for individual Stark components, the same value of Γ_n^{CR} should be used in our equation (25) for each Stark component of the given n. In the opposite case when the l-splitting is dominant, bound fractions ω_{nl} of the individual nl-states must be evaluated. For the nl-states the tunneling probabilities $\Gamma^{\text{tunn}}_{q=(nl)}$ are obtained by weighting of $\Gamma^{\text{tunn}}_{q=(n_1,n_2,m)}$, as explained in reference [33]. Note that, instead of using the approximate expression (25) of [33], we carry out the weighting (expression (23) of [33]) explicitly, omitting the linear Stark term in the expression (20) of [33]. This provides a better accuracy for $\Gamma^{\text{tunn}}_{q=(nl)}$.

Another important accuracy-increasing measure is the substitution into the expression (20) of reference [33] of the effective principal quantum number n^* in place of the integer n. In reference [33], n^* is introduced as $\gamma = 1/n^*$ for $Z_0 = 1$. In our notation this corresponds, for arbitrary Z_0, to

$$n^* = \frac{Z_0 e}{\sqrt{2a_0 E^0_{\text{bind}}}}.$$

Use of n^* allows to take into account the effect of the emitter-ion core electrons on the optical electron binding energy. We note, however, that in nonideal plasmas the optical electron binding energy is affected not only by the spatial distribution of the core electron densities inside the emitter ion, but also by the free-electron and ion spatial distribution *around* the emitter ion, *i.e.*, by plasma polarization. Therefore, in the present study we use n^* given by the expression

$$n^* = \frac{Z_0 e}{\sqrt{2a_0 E^{\text{eff}}_{\text{bind}}}}, \tag{26}$$

see equation (18) for $E^{\text{eff}}_{\text{bind}}$. The reduction in the binding energy due to the effect of surrounding particles is now accounted for. This results in additional substantial accuracy improvement.

In the case when $Z_\text{i} < Z_0$ the probability of tunneling is reduced significantly, since the volume available to the escaping optical electron in the NN ion potential well is relatively small. Thus, for an emitter ion immersed in plasma with $Z_\text{i} < Z_0$ the leading collectivization mechanism is overbarrier, and tunneling may be disregarded.

Numerical calculations performed using a non-equilibrium collisional-radiative kinetic code show that the tunneling tends to be unimportant for high n. Under broad variety of conditions we have observed that the tunneling escape dominates, compared to the overbarrier escape, for the $1s$, $2s$ and $2p$-states, whenever the perturber ions with $Z_\text{i} \geq Z_0$ are dominating the plasma composition. R_{tunn} was also found to exceed $R_{\text{crit.peak}}$ for some components of $n = 3$, 4 and 5 states, but the difference between R_{tunn} and $R_{\text{crit.peak}}$ in these cases was very small (the resulting variations in ω were less than 1%). For higher n the tunneling escape seems to be of no importance at all. Still, the expression (12) was used for all the numerical calculations presented below, *i.e.*, the tunneling for $Z_\text{i} \geq Z_0$ was never neglected.

4.6 Screening

As said in the introduction, the polarization of the surrounding plasma by the emitter ion [12] leads to the reduction of the binding energies of all the states n of the emitter ion by an amount ΔE introduced in expression (18) above. The highly-excited atomic (ionic) states with the isolated-ion binding energies $E^0_{\text{bind}} < \Delta E$ are eliminated, *i.e.*, replaced by the free-electron states. The energy reduction ΔE is approximately given by

$$\Delta E = Z_0 e^2 / R_\text{D}, \tag{27}$$

(see *e.g.* Refs. [12,34]), with the Debye screening radius R_D given by

$$R_\text{D}(N, T_\text{e}) = \sqrt{\frac{T}{4\pi e^2 \left(N_\text{e} + \sum Z_\text{i}^2 N_{Z_\text{i}}\right)}}.$$

The sum is over all the present ion species Z_i, with their respective densities denoted by N_{Z_i} (see footnote in Sect. 4.1). This expression is obtained in the assumption that both free electrons and ions participate in the screening of the emitter ion and of the removed optical electron.

For Debye screening of an ion which charge state does not change in time, the screening particle masses are of no importance, and thus the roles of electrons and ions in the screening are equivalent. However, the quantity ΔE, as defined by equation (18), gives the reduction of **ionization** energy due to screening. The ionization implies the temporal change of the test-ion charge state, and therefore the respective contributions of the surrounding ions and of the free electrons to ΔE are not equivalent. It should be

expected that the collectivized electron leaving the parent ion is still too fast to be screened by ions, and therefore only the free electrons can screen it while the ions can not. Similarly, only the free electron density "adjusts itself" when the emitter ion charge changes from $Z_0 - 1$ to Z_0. Taking this into account, we have found

$$\Delta E = \frac{e^2}{R_{\rm D}^{\rm e}} \left\{ 1 + (Z_0 - 1) \left(2 + \frac{\sum Z_{\rm i}^2 N_{Z_{\rm i}}}{N_{\rm e}} \right) \frac{R_{\rm D}}{R_{\rm D} + R_{\rm D}^{\rm e}} \right\}, \tag{28}$$

where

$$R_{\rm D}^{\rm e}\left(N_{\rm e}, T_{\rm e}\right) = \sqrt{\frac{T}{4\pi e^2 N_{\rm e}}} \tag{29}$$

is the Debye screening radius in the case of screening by free electrons only. In this work the expression (28) for ΔE is used.

To avoid any possible ambiguity, it should be emphasized that, while the reduction of the binding energies of the atomic (ionic) bound states in weakly-coupled plasmas is given by the expression (28), we do not use the Debye-Hückel *potential* $Z_0 e r^{-1} \exp(-r/R_{\rm D})$ as the binding one. The binding potential we use is the superposition of the bare Coulomb potentials of the parent ion, of the NN ion, and (in the next subsection) of the other surrounding particles[4]. As it has been already stressed in several reviews (see, *e.g.*, [12,18]), the Debye-Hückel potential can be used to assess neither the wavefunctions nor even the level shifts for the states with $E_{\rm bind}^0 \approx \Delta E$ since for these states (which have typical average radii $\langle r_n \rangle \approx R_{\rm D}/2$, see Ref. [12]) the presence of the individual perturbers within $\langle r_n \rangle$ from the parent ion is clearly of greater importance. Levels, which $E_{\rm bind}^0$ is larger but close to ΔE, lie close to the Debye limit and thus encompass many perturbing ions, since in the ideal or weakly-coupled plasmas there are many perturber ions inside a Debye sphere. Therefore, these levels are fully collectivized, forming a quasi-continuum, and thus the discussion of their exact binding energies is redundant anyway. The truly-bound states, on the other hand, have no perturbing ions within the distance $R_{\rm crit.peak}$ from the parent ion. $R_{\rm crit.peak}$ is several times larger than $\langle r_n \rangle$, as the comparison between the expressions (10) and (11) readily shows. Thus, the presence of perturbing ions within $\langle r_n \rangle$ from the emitter ion is indeed highly unlikely, and the binding energy reduction due to screening is described for the truly-bound states by (28) quite accurately.

[4] Of course, the bare ionic potential is Coulomb only *outside* the core electrons cloud, *i.e.*, at the distances from the nucleus that exceed significantly the core-electron wavefunction radii. In reference [22] we have explained in detail that, as long as the optical electron binding potential is considered at the distances about $r_{\rm class}$ or larger from the ion nuclei, both the parent ion and the perturber ions can indeed be treated reliably as pointlike. The short-range behavior of the optical-electron binding potential within the parent ion core determines, however, the optical electron binding energy $E_{\rm bind}^0$. In this work we use the accurate tabulated values of $E_{\rm bind}^0$ available in the NIST Atomic Spectra Database [35].

The approach here proposed is equally useful for the treatment of nonideal plasmas. Similarly to the ideal plasmas case, atomic states with the average radii $\langle r_n \rangle < a$ are weakly collectivized, states with $\langle r_n \rangle \gtrsim a$ are significantly collectivized, and states with $\langle r_n \rangle \gg a$ are screened by free electrons and ions (*i.e.*, eliminated). The only difference is that in strongly nonideal plasmas the number of free electrons in a Debye sphere is too small to allow for the screening, so the level elimination by screening occurs at radii $R_{\rm scr}$ larger than the Debye radius $R_{\rm D}$.

The analytical expression for the function $P_0\left(R\right)$, as given in reference [22], is valid for $\Gamma_{\rm ii}$ values up to 1. On the other hand, the Debye-Hückel approximation for ΔE, expression (28), breaks down at significantly lower values of $\Gamma_{\rm ii}$: it should not be used when there are less than, say, $10Z_0$ electrons in the Debye sphere, *i.e.*, when

$$\frac{4}{3}\pi N_{\rm e} R_{\rm D}^3 \leq 10 Z_0.$$

For $Z_0 = Z_{\rm i} = 1$ (neutral emitter in the plasma of singly-charged ions) this corresponds to $\Gamma_{\rm ii} \geq 0.036$. Thus, for plasmas with stronger coupling, $R_{\rm D}$ and $R_{\rm D}^{\rm e}$ are replaced in the expression (28) by larger radii $R_{\rm scr}$ and $R_{\rm scr}^{\rm e}$, respectively, while the other elements of the present theory remain valid and require no amendment.

It is clear that in plasma the screening sphere contains the number of free electrons that is much larger than the emitter ion parent charge Z_0. Therefore, to evaluate the effective statistical weights of the bound states in plasmas for $\Gamma_{\rm ii}$ values up to 1, we suggest taking the effective screening sphere radius $R_{\rm scr}$ using the relation

$$R_{\rm scr} = \max\left\{ R_{\rm D}, \left(\frac{30 Z_0}{4\pi N_{\rm e}} \right)^{1/3} \right\}. \tag{30}$$

This expression is used in all the calculations presented. To be consistent, in the cases when $R_{\rm scr} = \left(30 Z_0 / 4\pi N_{\rm e}\right)^{1/3}$ the electrons-only screening radius $R_{\rm D}^{\rm e}$ given by expression (29) must be replaced by $R_{\rm scr}^{\rm e} = R_{\rm scr}\sqrt{1 + \sum Z_{\rm i}^2 N_{Z_{\rm i}}/N_{\rm e}}$. This replacement preserves the continuity of the electrons-only screening radius as a function of macroscopic plasma parameters.

The effect of the binding energy reduction by the interaction with the free electrons can be, in nonideal plasmas, significantly more important than the Stark corrections to the binding energies. To illustrate this finding quantitatively, in the equation (22) we have varied artificially by $\pm 10\%$ the ΔE term (contained in $E_{\rm bind}^{\rm eff}$) and the linear Stark term. In the low-Z_0 plasmas with $\Gamma_{\rm ii} \approx 0.1$ the most abundant species have, roughly speaking, the levels $n \approx 3{-}10$ affected by the ESW reduction. Higher levels have $\omega \ll 1$, while lower levels have ω close to 1. It was found for these levels that the variation of ΔE elicits at least an order-of-magnitude stronger response in ω_n than the equivalent variation in the linear Stark shift coefficient.

It is also important to mention that the proper account for the reduction of the binding energies yields readily the correct asymptotic behavior of the bound fractions, namely, $\omega \to 0$ as $E_{\rm bind}^{\rm eff}\left(N_{\rm e}, T_{\rm e}\right) \to 0$. Indeed, if an atomic

state q with $E_{\rm bind}^{\rm eff} \to +0$ had a nonzero bound fraction ω_q, then at every $(N_{\rm e}, T_{\rm e})$ point where $E_{\rm bind}^{\rm eff}$ of any atomic state crosses zero the free electron density and the plasma thermodynamic potentials would have had discontinuities, which is obviously unphysical (see, *e.g.*, Ref. [36]).

4.7 Effects of the stochastic part of the potential of other perturbing particles

As explained in Section 4.2, a total perturbing potential acting on an emitter ion in plasma can be presented as a sum of three terms, namely,

(i) the NN ion potential,
(ii) the average (screening) part of the potential of OPP,
(iii) and the stochastic part of the potential of OPP.

In the previous subsections, the critical distances $R_{\rm crit.peak}$ and $R_{\rm tunn}$ between the emitter ion and the NN ion were determined taking into account the terms (i) and (ii) of the perturbing potential. We now consider the influence of the ionic part of the term (iii) of the perturbing potential on the values of $R_{\rm crit.peak}$ and $R_{\rm tunn}$.

For analyzing the effect of the term (iii) on $R_{\rm tunn}$ let us consider the values of the tunneling probability $\Gamma_q^{\rm tunn}(R)$. Up to now, we considered the tunneling between the potential wells of the parent ion and of a single perturbing ion (namely, the NN ion), in presence of screening. Introduction of the perturbing potentials of individual particles other than the NN ion produces two important effects. First, the tunneling may now occur into a different potential well (namely, into the NNN ion well). Second, the axial symmetry of the two-potential-well problem is broken, resulting in the mixing of the optical electron states from which the tunneling occurs. The second effect proves much more important than the first one. Indeed, from expression (12) of reference [22] it follows that in weakly-coupled plasmas the NNN ion is situated, on average, 1.5 times further from the emitter ion than the NN ion from the emitter ion (this remains quite accurate even for substantially nonideal plasmas with ion-ion coupling parameter values reaching 1). The probability of tunneling $\Gamma_q^{\rm tunn}(R)$ is extremely sensitive to R, thus the tunneling flux in the direction of the NNN ion is negligible compared to that in the NN ion direction. Thus, it is accurate to consider the tunneling only into the NN ion potential well.

The effect produced by the field $\mathbf{F}_{\rm OPP}$ of the other particles on the atomic wavefunctions is, however, significant. Previously, we have treated the tunneling from the Stark components $|n_1, n_2, m\rangle$ of the level n in the perturbing field $\mathbf{F}_{\rm NN}$ of the NN ion alone. The quantum numbers n_1, n_2, m are defined with respect to the perturbing field direction [24]. As long as the terms (i) and (ii) of the perturbing potential were considered, the perturbing electric field was parallel to the tunneling path, and, therefore, tunneling from the individual pure Stark components was considered. When the term (iii) is taken into account, this is no longer true. Indeed, $\mathbf{F}_{\rm OPP}$ is not parallel to $\mathbf{F}_{\rm NN}$. The Stark component wavefunctions $\langle \mathbf{r} \mid n_1, n_2, m\rangle$ do not depend on the field strength $F = |\mathbf{F}|$; they do, however, depend on the *direction* of the field. Thus, in the total field of the NN ion and other particles, $\mathbf{F} = \mathbf{F}_{\rm NN} + \mathbf{F}_{\rm OPP}$, the Stark-component wavefunctions are *rotated* in space with respect to their form in the field $\mathbf{F}_{\rm NN}$ alone. The rotation causes mixing of the Stark states,

$$|n_1, n_2, m\rangle = \sum_{n_1', n_2', m'} C_{n_1', n_2', m'}^{n_1, n_2, m} |n_1', n_2', m'\rangle ,$$

where $C_{n_1', n_2', m'}^{n_1, n_2, m}$ are the mixing coefficients and all $|n_1', n_2', m'\rangle$ belong to the same manifold n. The probability of tunneling from the mixed states is given by

$$\Gamma_{n_1, n_2, m}^{\rm tunn(mix)} = \sum_{n_1', n_2', m'} \left| C_{n_1', n_2', m'}^{n_1, n_2, m} \right|^2 \Gamma_{n_1', n_2', m'}^{\rm tunn}$$

[33], see also reference [32]. We have evaluated the coefficients $C_{n_1', n_2', m'}^{n_1, n_2, m}$ (the details of these calculations, being cumbersome, will be presented elsewhere), and found the mixing to be strong. We made available a table of mixing coefficients [37] for $n \leq 11$. The mixing results in a dramatic reduction of the spread of the tunneling probability values of the mixed Stark components compared to the pure ones, due to the strong increase in the probabilities of tunneling from the "blue" components ($n_1 > n_2$). In the examples of the ω calculations presented in this paper, the mixing effect on the tunneling probabilities was accounted for.

Let us now consider the effect of the term (iii) of the perturbing potential on $R_{\rm crit.peak}$. The surrounding ions (and, first of all, the NNN ion) affect the overbarrier escape of the optical electron from the emitter ion into the NN ion potential well by distorting the potential in which the overbarrier escape occurs. It is easy to see that in some cases the escape is hindered while in the others it is facilitated; thus in some individual atoms (ions) $R_{\rm crit.peak}$ is reduced while in the others it is increased. One can estimate the magnitude of the resulting changes in $R_{\rm crit.peak}$ by considering the effect produced by the NNN ion. We denote by r the distance between the emitter ion and the NN ion, by ρ the distance between the emitter ion and the NNN ion, and by θ the angle between the directions from the emitter ion to the NN ion and from the emitter ion to the NNN ion, $0 \leq \theta \leq \pi$. The value of $R_{\rm crit.peak}$ corresponding to a certain value of the angle θ is denoted by $\widetilde{R}_{\rm crit.peak}(\theta)$. Figure 2 shows the relative change in $R_{\rm crit.peak}$ due to the NNN ion effect, as a function of the angle θ. The results shown in Figure 2 were obtained for the average value of ρ, namely $\rho = 1.5r$, and for $Z_0 = Z_{\rm i}$. In plasmas the charges of the NN and NNN ions are generally similar, so the NNN ion charge was here also taken equal to $Z_{\rm i}$. Evidently, when $\theta \ll \pi/2$ (*i.e.*, the NNN ion is behind the NN ion) the potential barrier is lowered with respect to the optical electron energy level, the overbarrier escape is facilitated and $R_{\rm crit.peak}$ is increased. In the opposite case when $\pi - \theta \ll \pi/2$ (*i.e.*, the NN ion and the NNN ion are on opposite sides of the emitter ion) the potential barrier is raised with respect to the optical electron energy level, the overbarrier escape is

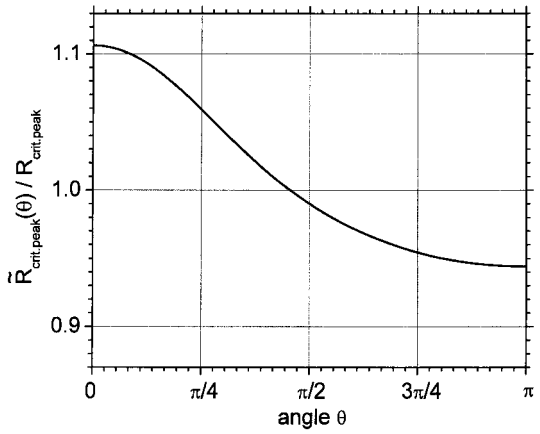

Fig. 2. Relative change in the $R_{\mathrm{crit.peak}}$ value due to the NNN ion effect.

hindered and $R_{\mathrm{crit.peak}}$ is decreased. We have shown [22] that the most likely values of θ are close to $\pi/2$. Figure 2 shows that in that region the change in $R_{\mathrm{crit.peak}}$ due to the NNN ion effect is quite small. Thus, the effect of the individual potential of the NNN ion (and of the stochastic part of the potential of the other perturbing particles) on $R_{\mathrm{crit.peak}}$ may be neglected.

5 Comparison with results found in literature

As a consequence of the problem great complexity, the results found in literature until now are obtained in very simple approximations. Namely, either only the effect of the NN ion is taken into account, using the ideal-plasma distribution of the distance to the NN ion (Ref. [13] and Sect. IV-e of Ref. [18]), or the effect of all the surrounding particles (including the NN ion) is reduced to the Uniform Local Microfield effect on the emitter ion (Ref. [18] – using Holtsmark ULM distribution [27], Ref. [21] – using APEX ULM distribution [38]), as will be further discussed below. Therefore, the comparison of our results to the published results provides an important insight into the effect of various assumptions made in literature.

The effect of the surrounding ions on the statistical weights of the bound states has been, since Unsöld's pioneering work [26], analyzed, most notably, by Gündel [13,14] and by Hummer and Mihalas [18]. The latter work also provides a detailed and comprehensive review of the progress in the field by the year 1988. An alternative approach, based on an ion cluster percolation, was suggested by Stein and Salzmann [29]. Below we will show that, using our present results, the empirical factor F that appears in the ESW calculations by Gündel [13, 14] and the empirical factor 2 that appears in the work by Hummer and Mihalas [18] may be replaced by well-defined physical quantities.

Gündel has conducted both the theoretical [13] and the experimental [14] studies of the reduction of the statistical weights of the individual levels of neutral argon, in a plasma of singly-ionized argon, *i.e.*, $Z_0 = Z_{\mathrm{i}} = 1$ case in our notation (note that in Ref. [13] the ion charges are introduced in a somewhat different way, namely, they are varied with distance to account for the optical-electron penetration into the core-electron cloud, *i.e.* for the deviation of the optical-electron unperturbed binding energy from its hydrogenic value). The NN ion approximation was used in reference [13] to account for the ion contribution to the bound-state statistical-weight reduction. The distribution function of the distance to the NN ion was taken in the ideal-plasma approximation.

Hummer and Mihalas, on the other hand, have used the ULM approximation and Holtsmark (*i.e.*, ideal-plasma) microfield distribution. The inaccuracy brought along by the use of the Holtsmark distribution in the nonideal plasmas has been since pointed out [21] and amended [21,39]. In the work by D'yachkov, Kobzev, and Pankratov [40], devoted to the plasma environment effect on the hydrogen spectrum near the series limit, the ULM approximation was used, too, but with the nonideal-plasma microfield distribution by Hooper [41].

In references [13,14,18] the role of free electrons in the reduction of the bound-state ESWs has been identified not with the binding energy reduction by screening, but rather with the level broadening by free-electron impacts. In our opinion, however, it is not *a priori* consistent to associate *both* the collectivization of an ionic state and the collisional removal of an electron from that state with the same process. There are two reasons for that. First, the inelastic processes caused by the electron impact produce transitions along the energy axis, while the collectivization is associated with the optical-electron motion in space only. In order to build a self-consistent picture of the kinetic processes in dense plasmas, these two kinds of processes must be clearly distinguished. Second, association of both the collectivization and the collisional ionization of a certain state with the same process (an electron impact) is likely to result in a double count. Indeed, consider for example a nonequilibrium plasma in which electrons are rapidly heated, so that the given ionic ground state is directly depopulated by electron impact ionization. A single act of electron impact ionization simply results in the ionization of a single ion, and certainly does not produce any additional ionization *via* the collisional broadening of that ground state. Therefore, we do not consider the electron-impact inelastic processes to be one of the causes of the bound-state statistical weight reduction.

On the other hand, the statistical weight reduction (brought along by the neighbor ion effects and by the *collective* free-electron effects) does affect the probabilities of the individual inelastic processes. For example, when an electron impact excitation occurs in an atom or ion immersed in a dense plasma, there is a finite probability that the final (upper) atomic state is collectivized while the initial (lower) state is truly bound. As said above, the electrons populating the collectivized states are considered free. Thus, an excitation into a collectivized state presents, in fact, an additional channel for electron impact *ionization*. The effects of electron-state collectivization on the collisional-radiative kinetics are further discussed in the next section.

Let us now return to a direct comparison of the theoretical results. The expressions for the ionic contributions to the statistical weight reduction, presented in references [13,18], involve the empirical factors F and 2, respectively. Using our expressions for the ESWs, these empirical factors can be replaced by the well-defined quantities. In reference [13] the NN approximation was used. Thus, the replacement of Gündel F factor (here denoted by $F_{\text{Gündel}}$) is readily accomplished: for the case $Z_0 = Z_\text{i} = 1$ considered in [13,14], we find that

$$F_{\text{Gündel}} \approx \frac{E^0_{\text{bind}}}{E^{\text{eff}}_{\text{bind}}} \equiv \frac{1}{1 - \Delta E\left(N_\text{e}, T_\text{e}\right) / E^0_{\text{bind}}}.$$

This relation ignores the differences between the ideal-plasma-limit NN distribution function used in [13,14] and the far more accurate temperature-dependent NN distribution function [22] that we use in the present work. It is important to stress that in [13,14] the empirical factor $F_{\text{Gündel}}$ was especially introduced to account for the other-ion effect on the ESW values. Here, we have shown that $F_{\text{Gündel}}$ is solely expressed through the relative reduction of the binding energy due to collective screening. Indeed, in the previous section we have shown that the collective, rather than the individual, effects dominate the other-ion influence on $R_{\text{crit.peak}}$ and, therefore, on ω.

In the case of Hummer and Mihalas' (HM) results [18] the direct comparison is far more complicated due to the extensive use of the ULM approximation in reference [18]. Briefly, the HM derivation goes as follows. The critical uniform local field F_{crit} for $n \leq 3$ is given by the expression (6) above. For $n > 3$ the ULM approximation suggests the presence of underbarrier overlap of the n and $n+1$ Stark manifolds (see Sect. 3). HM suggest that due to this overlap the state n can no longer be considered bound, and, therefore, the field value at which the overlap occurs (which is the Inglis-Teller critical field, $F^{\text{IT}}_{\text{crit}} = Z_0^3 e n^{-5} a_0^{-2}/3$, see Sect. 3) is in this case the critical one. HM introduce a factor K_n that changes smoothly from 1 for $n \leq 3$ to $16n/3$ for $n \gg 1$, to make a continuous transition between the two cases. Thus, finally, in the HM approach

$$F^{\text{HM}}_{\text{crit}} = \frac{E^2_{\text{bind}}}{4 Z_0 e^3} K_n.$$

As said above, HM see the rapid electron migration in the overlapping level array as a criterion for collectivization. However, in our picture of motion along the energy axis *vs.* a motion along the spatial axis, the rapid motion of an electron between states of the same atom does not make it free, but only the rapid motion of an electron between the neighbor ions does.

The fraction of emitter ions in which the level n remains bound despite the influence of the surrounding-ion field is then given, in HM approach, by

$$\omega_n^{\text{HM, ions}} = \int_0^{\beta^{\text{HM}}_{\text{crit}}} P_{\text{Holts}}\left(\beta\right) \mathrm{d}\beta, \tag{31}$$

where $P_{\text{Holts}}\left(\beta\right)$ is the Holtsmark microfield distribution (see, *e.g.*, [27]), and

$$\beta^{\text{HM}}_{\text{crit}} = \frac{F_{\text{crit}}}{F_0} = \frac{F_{\text{crit}}}{e\left(\frac{4}{3}\pi \sum\limits_{Z_\text{i}} Z_\text{i}^{3/2} N_{Z_\text{i}}\right)^{2/3}} \approx \frac{F_{\text{crit}}}{\langle Z_\text{i}\rangle\, e\left(\frac{4}{3}\pi N^{\text{tot}}_\text{i}\right)^{2/3}}.$$

Here $N^{\text{tot}}_\text{i} = \sum\limits_{Z_\text{i}} N_{Z_\text{i}}$ is the total perturber density, and $\langle Z_\text{i}\rangle = \sum\limits_{Z_\text{i}} Z_\text{i} N_{Z_\text{i}} / N^{\text{tot}}_\text{i}$ is the mean perturber charge (note that the end of the first line of expression (4.35) in Ref. [18] has probably been truncated in print). A very interesting point is stressed in reference [18]: while the NN picture suggests an exponential decay of ω_n with an increase in n, the ULM picture suggests a much slower, power-law decay of ω_n. Indeed, in ideal single-perturber-species plasma, the NN picture gives

$$\omega_n = \exp\left\{-\frac{4}{3}\pi N_\text{i} R^3_{\text{crit}}\right\} = \exp\left\{-const_1 \times n^6\right\},$$

while the ULM picture gives

$$\omega_n^{\text{HM, ions}} = \int_0^{\beta^{\text{HM}}_{\text{crit}}(n)\to 0} P_{\text{Holts}}\left(\beta\right) \mathrm{d}\beta = const_2 \times n^{-15},$$

as $n \to \infty$. Here we have found the following explanation for this discrepancy: while it is easy to see that indeed the probability for the *nearest* perturber ion to produce at the emitter-ion location a very weak field $F < F_{\text{crit}}\left(n\right) \ll F_0$ decreases exponentially as $F_{\text{crit}}\left(n\right) \to 0$, the probability for *all* perturber ions to produce such a field decreases much slower, namely, according to a power law. This is due to the possibility of a near-complete cancellation between the individual-ion fields at the emitter-ion location. The very weak local microfields, $F \ll F_0$, are produced therefore not by the perturber configurations in which there are no ions close to the emitter, but rather by the configurations in which the fields produced by the individual perturber ions at the emitter location nearly cancel each-other. Evidently, in the configuration where there are several perturber ions within the critical distance R_n (or possibly even within $\langle r_n\rangle$) from the emitter, the emitter optical electron is certainly collectivized, regardless of the fact that at the emitter-core location the perturber-ion fields nearly cancel out. Thus, we reach the conclusion that the non-exponential decay of ω_n at large n predicted by the ULM approximation is not a true physical effect, but is rather an artifact of the ULM approximation. The true physical behavior is, therefore, described by the exponential decay of ω_n at $n \to \infty$ (or, strictly speaking, at $n^* = Z_0 e / \sqrt{2 a_0 E^{\text{eff}}_{\text{bind}}} \to \infty$), as predicted correctly by the NN approximation.

In the opposite limit of relatively strongly-bound states, $\omega_n \gtrsim 0.1$ (*i.e.*, $\beta^{\text{HM}}_{\text{crit}} \gtrsim 1$), the integral (31) is approximated in reference [18] by

$$\omega_n^{\mathrm{HM,\,ions}} = \exp\left\{-\frac{4}{3}\pi \times 16\left(\frac{Z_0^{1/2}e^2}{K^{1/2}E_{\mathrm{bind}}}\right)^3 \times \frac{\sum\limits_{Z_\mathrm{i}} Z_\mathrm{i}^{3/2}\mathcal{N}_{Z_\mathrm{i}}}{\mathcal{V}}\right\} = \prod_{Z_\mathrm{i}} \exp\left\{-\frac{4}{3}\pi N_{Z_\mathrm{i}} \times 2\left(\frac{2Z_0^{1/2}Z_\mathrm{i}^{1/2}e^2}{K^{1/2}E_{\mathrm{bind}}}\right)^3\right\}, \tag{32}$$

where $\mathcal{N}_{Z_\mathrm{i}}$ are the absolute numbers of the perturber ions of the respective charge in the volume $\mathcal{V}$ considered. This is, up to the empirical factor of 2, the NN-approximation expression[5]

$$\omega_n = \prod_{Z_\mathrm{i}} \exp\left\{-\frac{4}{3}\pi N_{Z_\mathrm{i}} R_{\mathrm{crit.unif}}^3\right\},$$

with

$$R_{\mathrm{crit.unif}} = \sqrt{\frac{4Z_0Z_\mathrm{i}e^4}{KE_{\mathrm{bind}}^2}} = \sqrt{\frac{Z_\mathrm{i}e}{F_{\mathrm{crit}}^{\mathrm{HM}}}},$$

which is the distance at which the NN ion produces the field $F = F_{\mathrm{crit}}^{\mathrm{HM}}$. For $K \approx 1$ (low n), the empirical factor 2 in reference [18] amends partially for the inaccuracy introduced there by the simplifying approximation of the uniformity of the NN-ion field. Taking E_{bind} given by (2), and $Z_0 = Z_\mathrm{i}$, we find

$$R_{\mathrm{crit.unif}} = 4n^2a_0/Z_0,$$
$$R_{\mathrm{crit.peak}} = 6n^2a_0/Z_0.$$

Thus, we find that the use of the factor of $1.5^3 = 3.375$ restores the ideal-plasma NN-approximation result for hydrogen. The empirical factor of 2, used instead of this factor by HM, produces the results for low n and high ω that are still not far from the NN approximation predictions. Thus, HM (Ref. [18], see also Refs. [17,23,39]) have probably reached the best accuracy possible within the framework of the ULM approximation. It is the oversimplifying basic assumption of the local-field uniformity that limits the accuracy of any treatment based on it, in comparison to the treatment based on a more detailed microscopic plasma picture developed in the present work.

6 Discussion

6.1 Dependence of ω on the plasma parameters

As shown above, the fraction ω_q of ions in which the state q may be considered bound is determined by expression (17). It is important to realize that the two functions comprising this expression (namely, R_q as a function of the quantum numbers of the state q, and $P_0(R)$ as a function of the macroscopic plasma parameters) describe the different aspects of the physics involved, providing an effective separation between the atomic physics and the statistical mechanics of an atomic-state perturbation by the plasma environment. Indeed, the function $P_0(R)$ only describes the statistics of plasma particles spatial distribution, and does not depend on the state q of the emitter ion at all[6]. The function R_q, on the other hand, mostly depends on the shape of the optical-electron wavefunction. There still remains, however, a dependence of R_q on the macroscopic plasma parameters. As it was shown above, $R_q = R_{\mathrm{crit.peak}}$ in the majority of cases. The quantity $R_{\mathrm{crit.peak}}$ depends, besides the quantum numbers of the state q, on the perturber charge Z_i, on the emitter parent charge Z_0, and on $\Delta E(N_\mathrm{e}, T_\mathrm{e})$. The charges Z_0 and Z_i are not macroscopic plasma parameters. Namely, Z_0 is an external parameter of the problem, while Z_i plays a role of an index (see expression (17)). Thus, it is only through the binding-energy-reduction value ΔE that the critical distance R_q is influenced functionally by the macroscopic plasma parameters. Having this in mind, let us now describe qualitatively the dependence of ω_q on the plasma temperature and on the plasma ion densities N_{Z_i}. The primary dependence of ω_q is, evidently, on the ion density, *i.e.* on the characteristic interionic distance a. Indeed, ω_q changes from $\omega_q \approx 1$ for $a > 2R_q$ to $\omega_q \ll 1$ for $a < R_q/2$, while R_q itself is only weakly dependent (*via* ΔE) on the plasma density. Thus, ω_q is always a monotonously-decreasing function of all N_{Z_i}.

The dependence of ω_q on the temperature is, on the other hand, far more subtle. There are three main mechanisms of this dependence, sometimes producing opposite trends. The primary mechanism is the dependence of the plasma ion-composition N_{Z_i} on T. Indeed, at fixed total ion density $N_\mathrm{i}^{\mathrm{tot}} = \sum N_{Z_\mathrm{i}}$, the average perturber charge $\langle Z_\mathrm{i}\rangle = \sum Z_\mathrm{i}N_{Z_\mathrm{i}}/N_\mathrm{i}^{\mathrm{tot}}$ increases with T_e. More highly-charged perturber ions collectivize the emitter optical electron at larger critical distances R_q, thus reducing ω_q as T_e grows. This effect is the most important one, unless the plasma is almost fully-ionized. In the latter case, the nuclei are the dominant perturbers, and T_e no longer influences ω_q through the plasma ion composition. Another mechanism of the ω_q dependence on T_e is brought along by an increase in ΔE (decrease in the binding energy) as the plasma becomes less ideal, *i.e.*, as T_e decreases. Larger T_e correspond to smaller ΔE, larger $E_{\mathrm{bind}}^{\mathrm{eff}}$, smaller R_q, and thus larger ω_q, in contrast to the previous mechanism that tends to reduce ω_q with T_e. The effect of this mechanism is usually masked by the previous one, unless, as here said, the plasma is close to a complete ionization. This is rather unexpected: the nonideality effects, like the dependence of ω_q on ΔE, are usually manifested at lower temperatures. Finally, the third source of the ω_q temperature dependence is the distribution function $P_0(R)$. In this case the dependence on T is different for neutral emitters ($Z_0 = 1$) and for charged emitters ($Z_0 > 1$). For $Z_0 > 1$, at $R < a$ the direct emitter-perturber Coulomb repulsion is important, which at lower T_i hinders the close emitter-

[5] There seems to be a misprint on the line 1, column 2, page 812 of reference [18]: the cross-reference should point to the expression (4.16) rather than (4.67).

[6] $P_0(R)$ is strictly independent of q when $U_{\mathrm{NN}}(R)$ given by the expression (16) is used. However, there is a weak dependence of $P_0(R)$ on q when the correction term $\tilde{Z}_\mathrm{t}(R)$ is used in $U_{\mathrm{NN}}(R)$; see the explanation in reference [22].

perturber approaches, *i.e.*, increases $P_0(R)$ in the $R < a$ domain. Thus, at $\omega_q \approx 1$ there exists an additional mechanism bringing ω_q closer to 1 as the temperature decreases. In the $R > a$ domain, on the other hand, the attraction to the excess electrons located within the distance R from the emitter becomes more important (see Ref. [22]), and thus for $\omega_q \ll 1$ there is an additional decrease in ω_q as the ion temperature decreases. For the neutral emitter, however, the direct emitter-perturber repulsion is absent (except at the very small distances), and, therefore, $P_0(R)$ decreases with T_i throughout the entire R range. The importance of this effect increases with the plasma nonideality. In the weakly-coupled plasmas, *i.e.* at $\Gamma_\mathrm{ii} \lesssim 0.1$, the effect is typically less than 1% in magnitude. However, it becomes substantial as Γ_ii approaches unity.

In Figure 3 we present examples of the calculated bound-fraction values. The calculations were performed for LiI and LiII in a lithium plasma at temperature $T_\mathrm{e} = T_\mathrm{i} = 5$ eV. The collisional-radiative equilibrium plasma composition was determined using a kinetic code we have developed. It is easy to check that for LiI at $R = R_\mathrm{crit.peak}$ the linear Stark splitting exceeds the splitting on l for $n > 6$, and for LiII – for $n > 3$. However, to avoid cluttering the plots, the l-dependence of ω is only shown for LiI $1s^2 2l$ configurations. Figure 3 illustrates the smooth decrease of the bound fraction from 1 to 0 with the increase in the ion density. It is easy to see that the primary role in the bound-fraction reduction is played by the over-barrier escape. The tunneling escape has some effect only for $n = 1$, 2 and 3 levels, and even then – a rather weak one. Note also that, in order to ensure the continuity of the derivatives of ω_q with respect to N_{Z_i}, N_e, and T, we recommend in the equations (12) and (30) to approximate the function $\max(x_1, x_2)$, where $x_1 > 0$ and $x_2 > 0$, by the smooth function $\left(x_1^k + x_2^k\right)^{1/k}$ where $k \gg 1$.

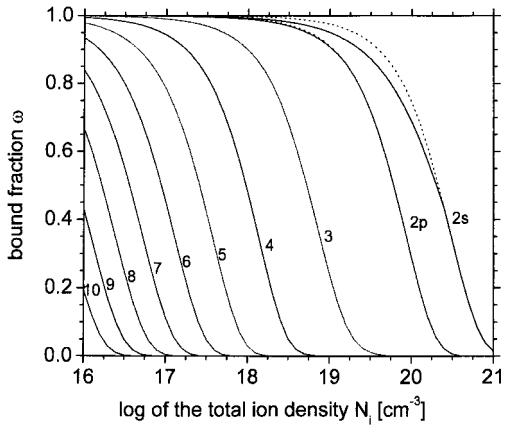

(a)

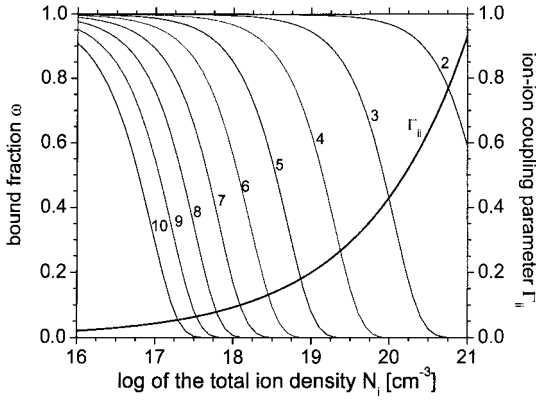

(b)

Fig. 3. (a) Bound fractions of LiI states with $n \leq 10$ at $T_\mathrm{e} = T_\mathrm{i} = 5$ eV. Numbers besides the lines denote the corresponding n values; splitting on l is shown for $n = 2$ only. Solid lines show the bound fractions evaluated using $R_q = \max\{R_\mathrm{crit.peak}, R_\mathrm{tunn}\}$. Dotted lines show the bound fractions evaluated using $R_q = R_\mathrm{crit.peak}$ (no tunneling). (b) Bound fractions of LiII states at $T_\mathrm{e} = T_\mathrm{i} = 5$ eV. Numbers besides the lines denote the corresponding n values. Thin lines show the bound fractions evaluated using $R_q = \max\{R_\mathrm{crit.peak}, R_\mathrm{tunn}\}$. Thick line shows the ion-ion coupling parameter Γ_ii given by expression (15). Here $Z_0 = 2$, and the dominant perturber at this temperature is $Z_\mathrm{i} = 1$.

6.2 Effects of electron-state collectivization on plasma kinetics

The development of a general model for electron states in plasmas and the derivation of high-accuracy expressions for the determination of the ESW of atomic (ionic) bound states in plasmas, as described above, make possible a substantial progress in two important fields. First, an unambiguous determination of the equilibrium plasma composition and properties becomes possible. Indeed, the ω_q values derived here can be readily utilized in the framework of the ESW formalism [20] to evaluate the free electron density N_e (and thus also the transport coefficients), partition function, thermodynamic potentials, Rosseland opacities, abundances of various ionization stages, and energy-level population densities in plasmas.

Second, the introduction made here of a rigorous classification of electron states into three types (bound, collectivized, and free), together with the derivation of the expressions for ω and ΔE, make now possible the study of the collisional and radiative kinetics in dense plasmas, equilibrium as well as transient, without the use of the traditional oversimplifying assumptions (namely, the assumptions of an identical environment for all atoms and of an identical level scheme for all atoms). In transient plasmas, the distinct consideration of the three types of electron states, and the proper account for the partial collectivization of the ionic states in an ensemble of ions, are crucial for an accurate description of the temporal evolution of plasma composition and atomic level populations. As an illustration, let us consider the three-body recombination process in a dense plasma. In the traditional Lowered-Ionization-Threshold approximation the three-body recombination proceeds predominantly into the highest surviving bound states, thus, the choice of the ionization threshold in the LIT approximation has a strong impact on the recombination dynamics predicted. In reality, the three-body recombination process is simply a Coulomb collision of two free electrons in an

external potential produced by a nearby ion, where as a result of the collision one of the electrons ends up in a bound state. In plasmas, only in a fraction ω_n of atoms (ions) the given state n is bound. The fraction ω_n goes to zero rapidly with n. Thus, the three-body recombination populates mostly the collectivized states, and only a small fraction $\sim \omega_n$ of the three-body recombination events going into the level n result in a true recombination (*i.e.*, in a reduction of the number of free electrons by 1). On the other hand, the collisional *deexcitation* event which brings an electron from a collectivized state down to a bound state reduces the number of free electrons by 1, thus contributing to the total *recombination* rate. The inverse process – a collisional excitation into a collectivized state – contributes to the electron impact ionization rate (see previous section). To summarize, the collectivization of the ionic states brings along a new class of kinetic effects, namely, the transitions involving the collectivized states. These transitions can play an important role in the formation of the ionization stage composition in transient plasmas. The results we have obtained, using the present approach, for the rates of kinetic processes and for the detailed-balance relations will be reported in detail in a separate paper [42].

In the cases where the results of the present work will be utilized for the treatment of the individual emitter-ion states that are characterized by the orbital angular quantum number l of the optical electron, especially for the states for which the $1-\omega$ values are not small, it must be realized that at the distances $R \sim R_{\rm crit.peak}$ from the NN ion the spherical symmetry of the parent binding potential is strongly perturbed, and l is no longer conserved. This can result, for example, in a significant increase in the probabilities of the dipole-forbidden transitions involving the affected state. Such changes in the matrix elements for atomic transitions occur for transitions between two bound states, as well as for the transitions involving collectivized or free-electron states. Thus, the collectivization of atomic states and the change in atomic matrix elements are two distinct effects produced by the dense plasma environment. The effects of the plasma environment on the matrix elements for collisional and radiative transitions in the atoms or ions are outside the scope of this work. These effects are considered, for example, in references [12,19, 43,44]. We note, however, that the statistical description of the perturbation of atomic states by neighbor particles in plasmas, developed in the present work, provides a natural framework for the incorporation of the plasma environment effects on the matrix elements into a general picture of dense plasma kinetics.

6.3 Conclusion

In literature, up to now, application-specific approximations were used to describe the different aspects of the dense-plasma physics: plasma ionization composition and bound state populations, plasma emission in lines and in continuum, spectral line broadening, plasma atomic physics, equation of state, optical properties, and transport coefficients. That is, for different applications different definitions of "bound" *vs.* "free" electron states were used, thus precluding a consistent description of a variety of plasma phenomena. The main reason for such inconsistency is the absence, until now, of an adequate description for the atomic states that are strongly perturbed by the neighbor particles. Indeed, due to the strong variation of the local microscopic conditions for individual atoms of the same kind, the same quantum state in individual atoms can be found in various degrees of perturbation, from almost unperturbed to effectively free.

The approximation most commonly used today is the traditional Lowered-Ionization-Threshold approximation, developed originally for the dilute weakly-coupled plasmas. In the LIT approximation all the plasma atoms are assumed to be found in identical microscopic conditions. The approximation is based on the separation of the electron states into bound (to a single ion) states below the LIT, and the free-electron states above the LIT. In the dilute plasmas, the perturbed states have sufficiently high principal quantum numbers and sufficiently low population densities for the exact value of the LIT to be not very important. Still, even for dilute plasmas, the LIT approximation yields a discontinuous free energy as a function of density and temperature, which is unphysical.

At the same time, a far more physical approach exists, based on the Effective Statistical Weights of the bound states decreasing smoothly to zero with the increasing probability of the strong perturbation of the respective bound states by the surrounding particles. Unlike the LIT approximation, the ESW approach is applicable to both dilute and dense plasmas. Although first proposed over 30 years ago, the ESW formalism has been up to now utilized systematically only in equation-of-state and opacity calculations for the stellar interiors [20]. The main reason for that was the absence, until now, of an accurate expression for the bound fractions ("occupation factors") ω of the atomic and ionic states. Indeed, the values of ω obtained using various approximations found in literature are in a strong disagreement with each-other (see, *e.g.*, Tab. I in Ref. [21]). Moreover, no method for direct experimental measurement of ω has been proposed so far.

In the present work, based on the ESW formalism, we have developed a description of the atomic (ionic) states that accounts for the collectivization of the atomic states by the surrounding ions and for the disappearance of the high (fully collectivized) states due to the screening by free electrons and ions. The electron states are divided into three distinct types: bound, collectivized, and free. The free electron density $N_{\rm e}$ includes both collectivized and the free electrons, as the electrons in states of both types can move between the ions in plasma without going through inelastic transitions. Both the collectivized and the free electrons participate in the conduction of heat and current.

Within the framework of this description, we have studied in detail the overbarrier and the tunneling mechanisms of the optical-electron escape from the emitter ion, and have derived accurate expressions for ESWs of atomic and ionic states. These expressions for ESW are based on detailed analysis of the distribution of individual

perturber particles around the emitter ion. Both the collective and the individual effects of the perturbing particles on the emitter ion energy levels were accounted for.

Even the simple estimates provided in Section 3 show that a proper account of the shape of the potential barrier separating the potential wells of the parent ion and of the NN ion results in significant amendments in the values of important physical quantities (*e.g.* the bound fraction values, the tunneling probabilities, and the onset of the Stark manifolds overlap). The detailed study was carried out of the roles of various processes and effects (overbarrier escape, tunneling, Stark effect, electron impact, screening) simultaneously affecting atomic or ionic states in plasmas of a wide range of compositions, temperatures and densities. This not only allowed to obtain accurate expressions for the ESWs of bound states, but also to reveal the relative importance and the mutual effect of various factors that are shaping the spectrum of the optical-electron states in atoms and ions immersed in plasma.

We express our deepest gratitude to H.R. Griem for his helpful comments and suggestions. We are highly indebted to V.I. Fisher, L.P. Pitaevskii, and D. Salzmann for many fruitful discussions.

References

1. K. Nazir, S.J. Rose, A. Djaoui, G.J. Tallents, M.G. Holden, P.A. Norreys, P. Fews, J. Zhang, F. Failles, Appl. Phys. Lett. **69**, 3686 (1996).
2. K.G. Whitney, J.W. Thornhill, P.E. Pulsifer, J.P. Apruzese, T.W.L. Sanford, T.J. Nash, R.C. Mock, R.B. Spielman, Phys. Rev. E **56**, 3540 (1997).
3. N.C. Woolsey, B.A. Hammel, C.J. Keane, C.A. Back, J.C. Moreno, J.K. Nash, A. Calisti, C. Mossé, R. Stamm, B. Talin, A. Asfaw, L.S. Klein, R.W. Lee, Phys. Rev. E **57**, 4650 (1998).
4. M. Nantel, G. Ma, S. Gu, C.Y. Côté, J. Itatani, D. Umstadter, Phys. Rev. Lett. **80**, 4442 (1998).
5. J.E. Bailey, H.K. Chung, A.L. Carlson, D. Cohen, D.J. Johnson, P. Lake, J.J. MacFarlane, P. Wang, D.R. Welch, Phys. Rev. Lett. **82**, 739 (1999).
6. L. Aschke, S. Depierreux, K.G. Estabrook, K.B. Fournier, J. Fuchs, S. Glenzer, R.W. Lee, W. Rozmus, R.S. Thoe, P.E. Young, J. Quant. Spectrosc. Radiat. Transfer **65**, 23 (2000).
7. K. Eidmann, A. Saemann, U. Andiel, I.E. Golovkin, R.C. Mancini, E. Andersson, E. Förster, J. Quant. Spectrosc. Radiat. Transfer **65**, 173 (2000); K. Eidmann, U. Andiel, E. Förster, I.E. Golovkin, R.C. Mancini, R. Rix, A. Saemann, T. Schlegel, I. Uschmann, K. Witte, *Atomic Processes in Plasmas* XII, edited by R.C. Mancini, R.A. Phaneuf, AIP Conf. Proc. **547**, 238 (2000).
8. J.S. Wark, E. Wolfrum, A.M. Allen, P.D.S. Burnett, A.M. Machacek, S.J. Rose, C.L.S. Lewis, R. Keenan, R. O'Rourke, D.H. Kalantar, M.H. Key, B.A. Remington, T.W. Barbee Jr., A. Djaoui, in abstracts of *9th International Workshop on Radiative Properties of Hot Dense Matter*, Santa Barbara, CA, 2000.
9. W. Lochte-Holtgreven, *Plasma Diagnostics* (AIP Press, New York, 1995).
10. *Radiative Properties of Hot Dense Matter III*, edited by R.W. Lee, J. Quant. Spectrosc. Radiat. Transfer **58**, No. 4-6 (1997).
11. *Radiative Properties of Hot Dense Matter IV*, edited by R.W. Lee, J. Quant. Spectrosc. Radiat. Transfer **65**, No. 1-3 (2000).
12. H.R. Griem, *Principles of Plasma Spectroscopy* (Cambridge University Press, 1997).
13. H. Gündel, Beitr. Plasmaphys. **10**, 455 (1970).
14. H. Gündel, Beitr. Plasmaphys. **11**, 1 (1971).
15. G.B. Zimmerman, R.M. More, J. Quant. Spectrosc. Radiat. Transfer **23**, 517 (1980).
16. V.E. Fortov, I.T. Yakubov, *Physics of Nonideal Plasma* (Hemisphere publ., New York, 1989; in *Russian*: 1984).
17. W. Däppen, L. Anderson, D. Mihalas, Astrophys. J. **319**, 195 (1987).
18. D.G. Hummer, D. Mihalas, Astrophys. J. **331**, 794 (1988).
19. D. Salzmann, *Atomic Physics in Hot Plasmas* (Oxford Univ. Press, New York, 1998).
20. *The Opacity Project*, edited by M.J. Seaton (IOP publ., Bristol, 1995), Vol. 1.
21. C.A. Iglesias, F.J. Rogers, Astrophys. J. **443**, 460 (1995).
22. D.V. Fisher, Y. Maron, Eur. Phys. J. D **14**, 349 (2001).
23. D. Mihalas, W. Däppen, D.G. Hummer, Astrophys. J. **331**, 815 (1988).
24. L.D. Landau, E.M. Lifshitz, *Quantum Mechanics (non-Relativistic Theory),* 3rd edn. (Butterworth-Heinemann Publ., 1997).
25. G.M. Lankhuijzen, L.D. Noordam, Adv. At. Mol. Phys. **38**, 121 (1997).
26. A. Unsöld, Z. Astrophys. **24**, 355 (1948).
27. H.R. Griem, *Spectral Line Broadening by Plasmas* (Academic Press, New York, 1974).
28. D.R. Inglis, E. Teller, Astrophys. J. **90**, 439 (1939).
29. J. Stein, D. Salzmann, Phys. Rev. A **45**, 3943 (1992).
30. H.R. Griem, *Plasma Spectroscopy* (McGraw-Hill, New York, 1964).
31. M. Busquet, Phys. Rev. A **25**, 2302 (1982).
32. D. Fisher, Y. Maron, L.P. Pitaevskii, Phys. Rev. A **58**, 2214 (1998).
33. T.P. Grozdanov, R.K. Janev, Phys. Rev. A **17**, 880 (1978).
34. Ya.B. Zel'dovich, Yu.P. Raizer, *Physics of Shock Waves and High-Temperature Hydrodynamic Phenomena* (Acad. Press, New York, 1966).
35. `http://physics.nist.gov/cgi-bin/AtData/main_asd`
36. R.M. More, Adv. At. Mol. Phys. **21**, 305 (1985).
37. `http://plasma-gate.weizmann.ac.il/~fndima/mixing/mixing.html`
38. C.A. Iglesias, J.L. Lebowitz, D. MacGowan, Phys. Rev. A **28**, 1667 (1983); C.A. Iglesias, H.E. DeWitt, J.L. Lebowitz, D. MacGowan, W.B. Hubbard, Phys. Rev. A **31**, 1698 (1985).
39. A. Nayfonov, W. Däppen, D.G. Hummer, D. Mihalas, Astrophys. J. **526**, 451 (1999).
40. L.G. D'yachkov, G.A. Kobzev, P.M. Pankratov, J. Phys. B **21**, 1939 (1988).
41. C.F. Hooper Jr, Phys. Rev. **165**, 215 (1967).
42. D.V. Fisher, V.I. Fisher, Y. Maron, to be submitted to Eur. Phys. J. D.
43. W. Ebeling, A. Förster, V.E. Fortov, V.K. Gryaznov, A.Ya. Polishchuk, *Thermophysical Properties of Hot Dense Plasmas* (B.G. Teubner Verlagsgesellschaft, Stuttgart, 1991).
44. M.S. Murillo, J.C. Weisheit, Phys. Rep. **302**, 1 (1998).